DE83 005340

ORNL/TM-8587
Dist. Category UC-95d

Contract No. W-7405-eng-26

Engineering Technology Division*

FEASIBILITY OF AN UNCONVENTIONAL HEAT-FLOW-MEASURING TECHNIQUE TO DETERMINE COEFFICIENT OF PERFORMANCE ON INSTALLED HEAT PUMPS

V. R. Brantley

*Work sponsored by the Energy Division

Date Published - January 1983

Prepared by the
OAK RIDGE NATIONAL LABORATORY
Oak Ridge, Tennessee 37830
operated by
UNION CARBIDE CORPORATION
for the
DEPARTMENT OF ENERGY

CONTENTS

Page

LIST OF FIGURES v
LIST OF TABLES vii
NOMENCLATURE ix
ABSTRACT 1
1. INTRODUCTION 1
2. SUMMARY AND CONCLUSIONS 4
3. BACKGROUND 6
4. EXPERIMENTAL PROGRAM AND EQUIPMENT 10
4.1 Temperature and Velocity Measurements 10
4.2 Equipment and Procedures for the Carrier Test Series 11
4.3 Equipment and Procedures for the GE Test Series 13
4.4 Assessment of Measurement System Error 15
5. CARRIER HEAT PUMP TESTING 17
6. GE HEAT PUMP TESTING 23
7. EVALUATION OF TEST DATA 27
7.1 Normalized Temperature Difference Variation 31
7.2 Effect of Temperature Sensor Configuration on Accuracy ... 32
7.3 Error Direction 34
7.4 Estimated Accuracy in Field Applications 34
8. RECOMMENDATIONS 37
REFERENCES 38
APPENDIX. COP METER – THEORY OF OPERATION AND PROTOTYPE DESIGN ... 39

LIST OF FIGURES

Figure		Page
3.1	Steady-state system with four discrete fluid streams	7
3.2	Typical heat pump indoor unit	8
4.1	Return and supply air thermocouple grids	11
4.2	Carrier heat pump indoor unit and supply duct	12
4.3	Carrier heat pump instrumentation	12
4.4	GE heat pump indoor unit and supply duct	13
4.5	GE heat pump instrumentation	14
5.1	Carrier supply duct air velocity data	19
5.2	Carrier supply duct air temperature data, refrigerant heating mode	20
5.3	Carrier supply duct air temperature data, resistance heating mode – high heater power level	21
5.4	Carrier supply duct air temperature data, resistance heating mode – low heater power level	22
6.1	GE supply duct air velocity data and refrigerant heating mode air temperature data – high fan speed	24
6.2	GE supply duct air temperature data, resistance heating mode – high fan speed	25
7.1	Carrier indoor unit and supply duct viewed from a point downstream in the supply duct	28
7.2	GE indoor unit and supply duct viewed from a point downstream in the supply duct	29
7.3.	Effect of dissimilar temperature profiles for resistance and refrigerant heating modes on heat flow in branch ducts	35
A.1	COP meter flow schematic	41
A.2	Prototype COP meter circuit design	42

LIST OF TABLES

Table		Page
2.1	Summary of the proposed heat flow measuring technique accuracy in the laboratory	5
5.1	Effect of fan speed, resistance heater power level, and distance of supply air temperature sensors from indoor unit on accuracy of the proposed heat flow measuring technique for the Carrier test series	17
6.1	Effect of resistance heater power level and distance of supply air temperature sensors from indoor unit on accuracy of the proposed heat flow measuring technique for the GE test series	23
7.1	Summary of supply air velocity and temperature data	30
7.2	Normalized temperature difference variation (standard deviation/mean temperature difference) for both test series	31
7.3	Error analysis of the proposed heat flow measuring technique based on the parametric investigation conducted in the laboratory	33

NOMENCLATURE

$\dot{Q}$	heat flow rate
$\dot{m}$	air mass flow rate
C_p	constant pressure specific heat
ΔT	temperature difference between entering and exiting air streams
V	air stream velocity
ρ	air density
A	duct cross-sectional area
K	proportionality constant

FEASIBILITY OF AN UNCONVENTIONAL HEAT FLOW MEASURING TECHNIQUE TO DETERMINE COEFFICIENT OF PERFORMANCE ON INSTALLED HEAT PUMPS

V. R. Brantley

ABSTRACT

Tests were performed on two split residential heat pump systems in the laboratory to determine the suitability of an unconventional heat flow measuring technique proposed for use in an instrument that determines the coefficient of performance of installed heat pumps. This technique uses the ratio of measured heat flow to measured temperature difference in the resistance heating mode to calculate heat flow in the refrigerant heating mode from the measured temperature difference during normal heat pump operation. Distance of the supply air temperature sensor from the indoor unit and resistance heater power level were found to be significant parameters that could be controlled to minimize error. Accuracy of the proposed heat flow measuring technique on units in field service was judged to be within 5%.

1. INTRODUCTION

Coefficient of Performance (COP) of a heat pump is defined for the heating mode as the ratio of heat supplied to energy required, using consistent units for the numerator and the denominator. A satisfactory instrument for measuring COP of installed heat pumps is not now available. Such a device is desirable for two reasons:

1. A data base of heat pump performance could be generated from measurements on units operating in field service. This empirical data could supplement or replace the estimated performance data currently used for energy consumption and power generation evaluations.
2. Periodic checks of heat pumps by dealers or utility representatives could be a valuable troubleshooting procedure. This instrument would make it possible to identify malfunctions that degrade performance but are not of sufficient severity to render the heat pump totally inoperative.

This instrument should be portable, reliable, rugged, reasonably accurate, simple to operate, and relatively inexpensive.

While electrical power input can be measured accurately with available instrumentation, measuring heat flow requires more sophisticated instrumentation and is subject to a high degree of probable error. The objective of this investigation was to determine the feasibility of using an unconventional heat flow measuring technique in a COP meter that would have the aforementioned qualities.

This proposed heat flow measuring technique minimizes the level of instrumentation required by using a procedure that calibrates the device in place for each unit to be tested. For a steady-state steady-flow system the heat flow equation may be written

$$\dot{Q} = \dot{m}\, C_p\, \Delta T \,. \tag{1.1}$$

If mass flow rate and specific heat of the air are constant, then the equation may be rewritten

$$\dot{Q} = K\Delta T \,. \tag{1.2}$$

The K factor for a system can be determined by measuring the air stream temperature difference generated across the indoor unit by a known heat source. For a conventional heat pump, temperature sensors placed in the return and supply air ducts are used to measure the air stream temperature difference. Resistance heating elements with a meter to measure the electrical power input will serve as a known heat source. Operating the heat pump in the resistance heating mode will thus make it possible to determine the K factor for each system. Once the system is calibrated, heat flow through the indoor unit in the refrigerant heating mode (i.e., using the heat pump itself rather than the resistance heaters) can be determined by measuring the air stream temperature difference and taking the product of this ΔT and the K factor.

Simplicity of this proposed heat flow measuring technique makes it well suited for use in a COP meter for two reasons:

1. The amount of instrumentation needed is considerably less than would be required for a more conventional heat flow measuring system.

2. Personnel using a device that operates on this principle would require no specialized knowledge of either thermodynamics or instrumentation practices.

A COP meter that uses this proposed heat flow measuring technique has been designed and is completely described in the appendix. This meter measures heat flow and power consumption, giving a ratio of the signals in such a way as to produce a displayed number that is the actual COP over the test interval.

2. SUMMARY AND CONCLUSIONS

Tests were run on two split residential heat pump systems in the laboratory to determine probable causes of error, means of minimizing error, and expected range of error. A summary of the experimental work is presented in Table 2.1. Error of the proposed measuring technique is strongly affected by two parameters:

1. supply air temperature sensor distance downstream from the indoor unit, and
2. resistance heater power level.

For every combination of fan speed and sensor distance in one test series, using a Carrier heat pump, magnitude of error decreases as temperature sensor distance from the indoor unit increases. Magnitude of error increases, however, as resistance heater power level increases. For each sensor distance in the other test series, using a General Electric Company (GE) heat pump, error is also a strong function of resistance heater power level. It is here concluded that the two parameters listed in the previous paragraph afford adequate opportunity for minimizing error with the proposed measuring technique. That the error is inversely related to distance from the indoor unit is quite logical; greater uniformity in temperature and velocity profiles occurs as the air stream moves down the duct. That the error is greater at higher resistance heater power levels is also quite reasonable; higher heater power levels generate greater supply air temperature variation.

From the experimental work and discussions with heat pump dealers concerning supply duct layout, it is concluded that the proposed heat flow measuring technique will be accurate to within 5% for 90% of the heat pumps currently in use if:

1. temperature sensors are used that measure the average temperature over the duct cross section,
2. the resistance heater power level is limited to 5 kW or less, and
3. the supply air temperature sensor is installed at least 1 m downstream of the indoor unit.

Table 2.1. Summary of the proposed heat flow measuring technique accuracy in the laboratory

Heat pump and grid position	Fan speed	Sensor distance from indoor unit (m)	Heater power (kW)	Maximum error[a,b] (%)	Error of averages[b,c] (%)
C-1	Medium	0.23	2.42	−12.5	−11.5
C-1	Medium	0.23	4.42	−15.8	−14.3
C-1	High	0.23	2.55	−14.0	−8.6
C-1	High	0.23	4.54	−14.0	−11.2
C-2	Medium	0.56	2.39	+3.1	+0.2
C-2	Medium	0.56	4.34	+5.6	+2.9
C-2	High	0.56	2.51	+4.4	+2.1
C-2	High	0.56	4.49	+6.8	+4.0
G-1	High	0.89	9.69	−2.8	−1.2
G-1	High	0.89	15.68	−7.4	−5.6
G-2	High	1.22 + transition	9.70	+5.6	+2.2
G-2	High	1.22 + transition	15.66	+6.7	+3.2

[a]The maximum error is the error of worst case refrigerant K vs resistance K.

[b]The "−" sign indicates that the refrigerant heat flow is understated and the "+" sign indicates that the refrigerant heat flow is overstated.

[c]The error of averages is the error using average refrigerant K vs average resistance K.

These estimates of accuracy on installed units are felt to be conservative, and it is considered likely that further experimentation will show that higher accuracies are possible.

3. BACKGROUND

Equation (1.1) is valid only for systems having a single heat transfer fluid stream that has uniform properties where it crosses the control boundary. If any of the terms on the right-hand side of the equation are not constants — that is, if any of the properties represented by these terms are not uniform across the fluid stream where it crosses the control boundary — then the correct mathematical relationship is

$$\dot{Q} = \sum_{i=1}^{n} V_i \rho_i A_i C_{p_i} \Delta T_i \ . \tag{3.1}$$

The difficulties in obtaining an integrated heat flow measurement such as that represented by Eq. (3.1), especially before the advent of low-cost high-speed digital computers, have undoubtedly influenced the development of conventional heat flow measuring techniques. Organizations such as the American Society of Heating, Refrigerating, and Air-Conditioning Engineers[1] and the American National Standards Institute[2] have drawn up standards that explicitly state ways and means by which heat flow is to be determined for systems using air at atmospheric pressure as a heat transfer fluid. Many of these standards have two basic goals:

1. to reduce the degree of variation in each property so that each term on the right-hand side of Eq. (3.1) is essentially a constant, and
2. to ensure that an acceptably accurate average value of each property is obtained.

Average value of each of the properties is used in Eq. (1.1). This general approach to heat flow measurement is, however, only an approximate method. The average values method attempts to equate the product of the sums with the sum of the products; a procedure that is not, in the general case, valid.

For example, consider a hypothetical system having four discrete fluid streams. Cross-sectional area, density, and specific heat are the same for all four streams, but either or both of the properties velocity and temperature difference may vary among the streams. Figure 3.1 illustrates four possible combinations of this system. Heat flow out of this

ORNL-DWG 81-4771

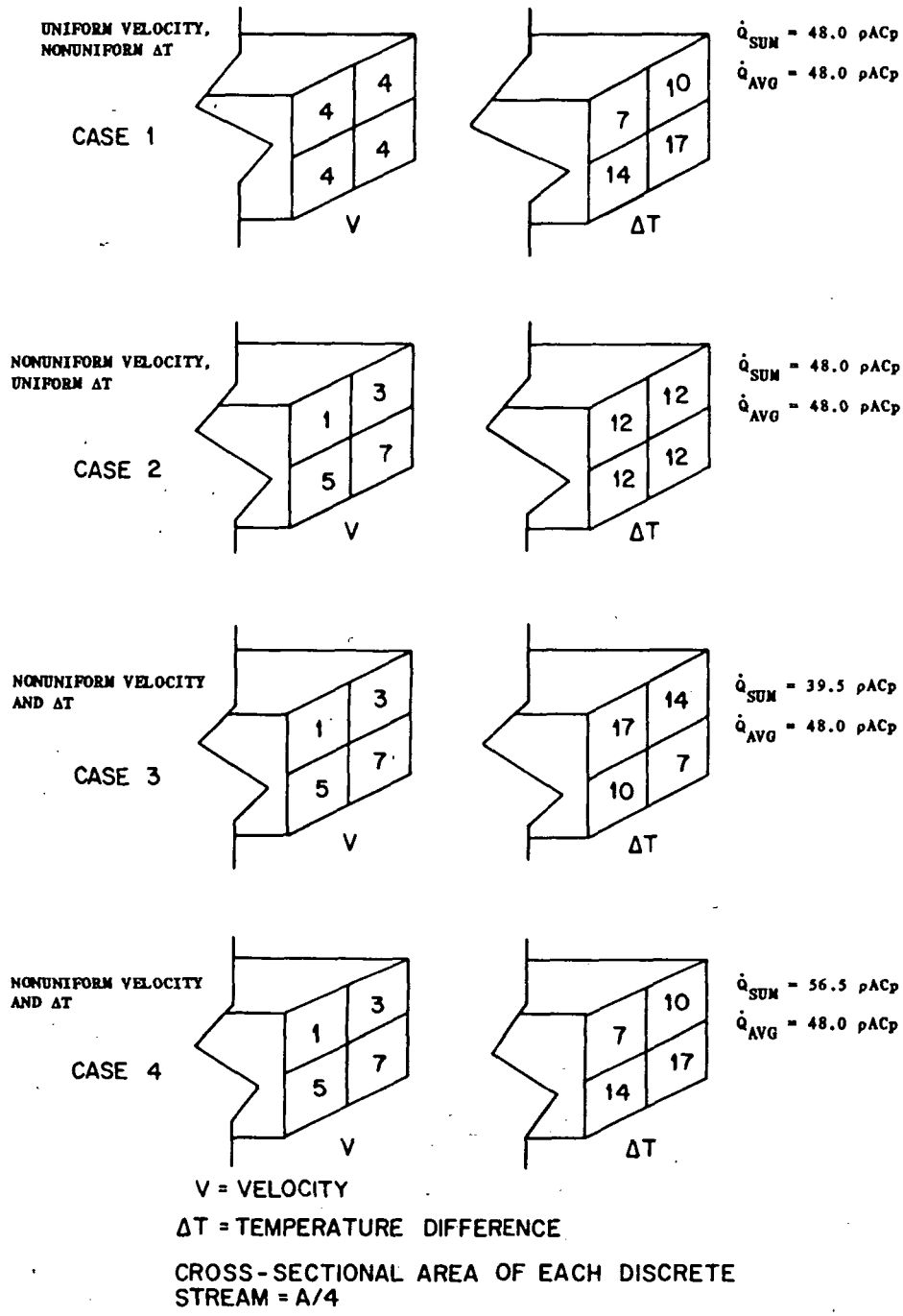

Fig. 3.1. Steady-state system with four discrete fluid streams.

sytem is calculated two ways:

$$\text{Summation method:} \quad \dot{Q}_{sum} = \rho \times \frac{A}{4} \times C_p \times \sum_{i=1}^{4} V_i \, \Delta T_i$$

$$\text{Average values method:} \quad \dot{Q}_{Avg} = \rho A C_p \times$$

$$\text{(average velocity)} \times \text{(average } \Delta T\text{)} \; .$$

Results of these calculations are listed to the right of Fig. 3.1.

The average values method produces correct answers in the first two cases because of the distributive law. For case 3, the average values method understates the actual heat flow by 21.5%; for case 4, it overstates the actual heat flow by 15.0%. Cases 3 and 4 also illustrate another fact — when the velocity and temperature difference profiles are skewed in the same direction, the average values method understates the actual heat flow; when the profiles are skewed in opposite directions, the average values method overstates the actual heat flow.

Figure 3.2 is a schematic of a typical heat pump indoor unit. Air velocity as it exits the blower is nonuniform because of the centrifugal action of the blower. Because the blower discharge face area is generally much less than the cross-sectional area of the supply duct, this adds to the velocity variation in the supply duct itself. In the resistance heating mode, the nonuniform air velocity over the resistance elements causes considerable variation in the air temperature as the air

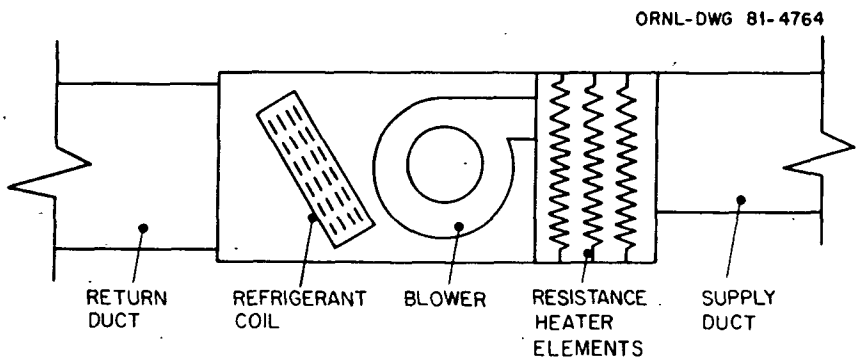

Fig. 3.2. Typical heat pump indoor unit.

enters the supply duct. Temperature variations, when the refrigerant coil is used, are much smaller. Latent heat accounts for most of the energy change in the refrigerant, so the refrigerant coil may be nearly isothermal. Heated air from the refrigerant coil is further mixed when it travels from the coil through the blower, so the air temperature is quite uniform when the air enters the supply duct. Temperature of the return air entering the indoor unit may be expected to be quite uniform. Air entering the return register is likely to be nearly isothermal at that point; subsequent mixing of this air when it travels through the return duct ensures near uniform temperature at the indoor unit.

Major sources of error for the proposed technique will be the velocity variation and temperature variation factors, which would be of primary concern for conventional heat flow measuring techniques. Using extended lengths of straight duct, such as is specified in standards for conventional heat flow measurement to effect near uniform velocity and temperature of the air stream, is not feasible in conjunction with a COP meter for installed heat pumps. Success of the proposed heat flow measuring technique is predicated on the assumption of constant mass flow rate and constant specific heat of the air stream during both the calibration and test periods. Total time required for calibration and testing would be on the order of 15 to 30 min, so this is a reasonable assumption to make provided that:

1. the state point of the return air is relatively constant,
2. the fan speed is unchanged, and
3. the duct damper and splitter positions are the same for the total time period.

4. EXPERIMENTAL PROGRAM AND EQUIPMENT

An experimental program was developed to determine the effect of three parameters on the accuracy of the proposed heat flow measuring technique. These three parameters were fan speed, resistance heater power level, and distance of the supply air temperature sensor downstream from the indoor unit. Testing was done on two split system residential heat pumps in the laboratory. Both heat pumps were instrumented so that total electrical power to the indoor unit and heat flux in the indoor unit refrigerant circuit could be monitored.

The proposed heat flow measuring technique is based on the relationship

$$\dot{Q} = K\Delta T \ .$$

For the resistance heating tests, $\dot{Q}$ was taken to be the total electrical power input to the indoor unit. For the refrigerant heating tests, $\dot{Q}$ was taken to be the sum of the electrical power input to the indoor fan and the heat delivered by the refrigerant circuit. Error of the proposed heat flow measuring technique is here defined as the percent difference between the resistance heating K value and the refrigerant heating K value at each set of parameter values; error was thus calculated using the equation

$$\% \text{ Error} = 100 \times (K_{resist} - K_{refrig})/K_{refrig} \ .$$

4.1 Temperature and Velocity Measurements

Thermocouple grids were used for the air side temperature measurements; thermocouple grid layouts are shown in Fig. 4.1. Calibration checks were made at two temperatures (0 and 23°C) using a mercury thermometer as a reference, and the thermocouples were judged to be sufficiently similar in response as to require no individual correction.

Supply air velocity measurements were made on both heat pumps at each grid position using a portable hot-wire anemometer. Ten points corresponding to the thermocouple locations at each grid position were sampled

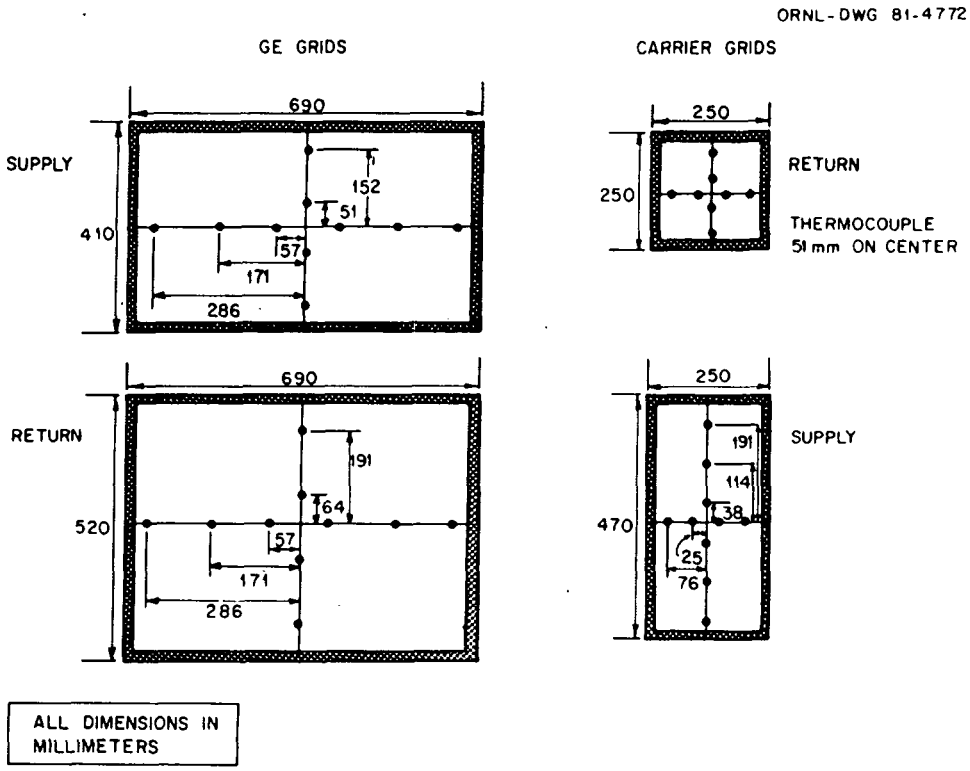

Fig. 4.1. Return and supply air thermocouple grids.

with the thermocouple grid removed and with only the fan operating. Velocities for medium and high fan speeds were measured on the first unit tested, and velocities for high fan speed only were measured on the second unit tested. These measurements were made solely to provide information on relative velocity variation among the three positions down the supply duct; they were not used for any air side heat flow calculations.

4.2 Equipment and Procedures for the Carrier Test Series

The first test series was run using a Carrier heat pump with a rated heating capacity of 10 kW. Figure 4.2 shows the locations at which the temperature and velocity measurements were made in the supply duct. Figure 4.3 shows the location of sensors used in the electrical, refrigerant, and air circuits and gives a brief description of the sensors used. A total of 40 tests were made using the Carrier heat pump, 24 in the resistance heating mode and 16 in the refrigerant heating mode. The data acquisition system (DAS) was programmed to scan and record data every 2 min

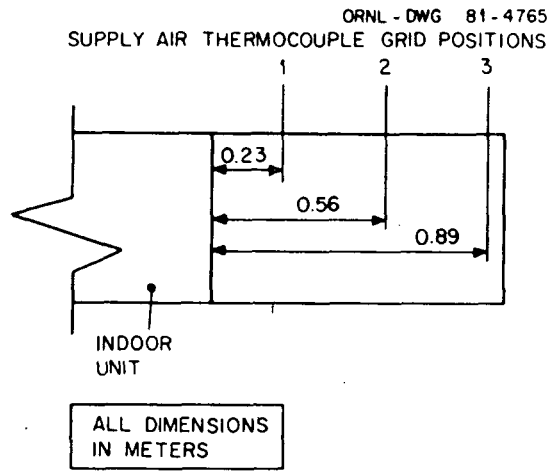

Fig. 4.2. Carrier heat pump indoor unit and supply duct.

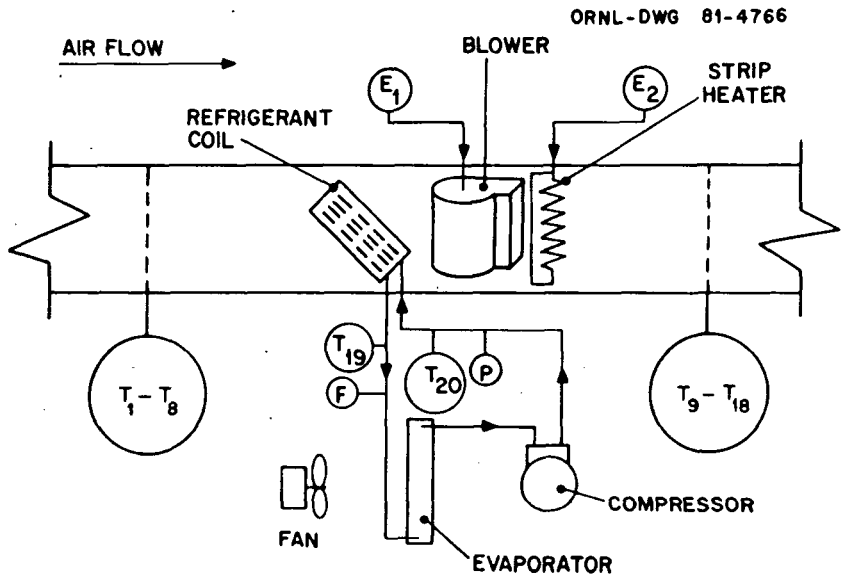

Point	Type*	Parameter	Sensor
E_1	0	Electrical power, indoor unit blower	Thermowatt converter
E_2	1	Electrical power, strip heaters	Voltmeter, ammeter
F	1	Refrigerant flow rate	Rotometer
T_1–T_8	0	Return air temperatures	Cu-Con thermocouples
T_9–T_{18}	0	Supply air temperatures	Ch-Al thermocouples
T_{19}	0	Refrigerant temperature exiting indoor unit	Ch-Al thermocouple
T_{20}	0	Refrigerant temperature entering indoor unit	Ch-Al thermocouple
P	1	Refrigerant pressure entering indoor unit	Bourdon-tube gauge

*0 = data logged automatically on DAS, 1 = data logged manually in log book

Fig. 4.3. Carrier heat pump instrumentation.

from the sensors indicated in Fig. 4.3. The heat pump was run under a set of conditions until the temperature measurements indicated that the heat pump had reached steady-state operation and the sensors had equilibrated to the new conditions.

A variable voltage power transformer was used to control the power input to the resistance heater elements. A power factor of 1 was assumed, and power to the strip heaters was calculated from voltage and current measurements made in the heater supply circuit. Electrical power to the fan was measured by a transducer monitored by the DAS. Heat output of the refrigerant circuit was manually calculated by the refrigerant enthalpy method using a combination of data from the DAS and manually logged data. Figure 4.3 shows the location and type of the sensors used to measure the necessary refrigerant properties for these calculations. Points P, T_{20}, T_{19}, and F provided the needed information.

4.3 Equipment and Procedures for the GE Test Series

The second test series was run using a GE heat pump with a rated heating capacity of 9.7 kW. Figures 4.4 and 4.5, respectively, show the

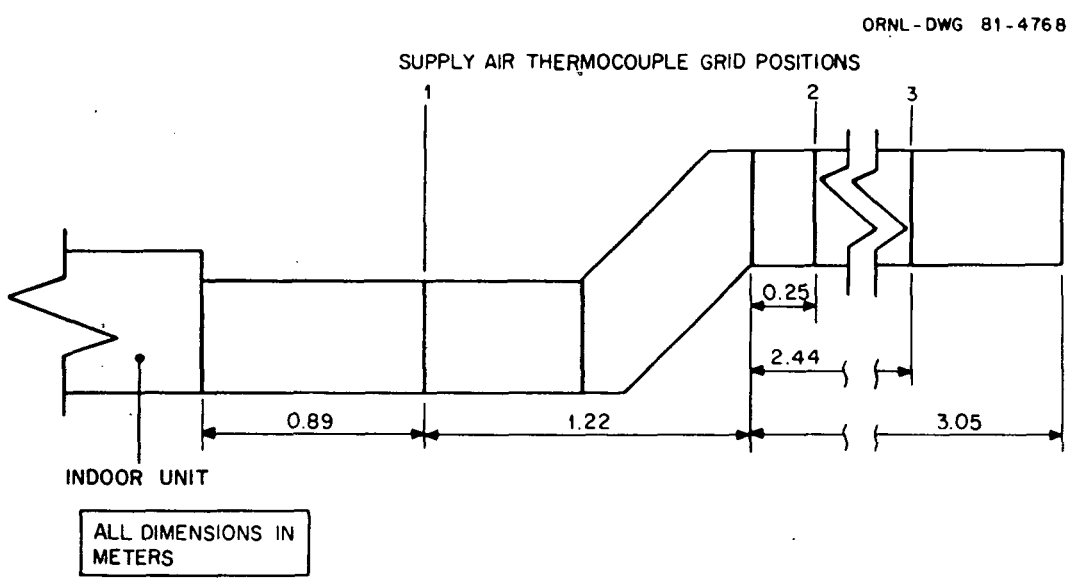

Fig. 4.4. GE heat pump indoor unit and supply duct.

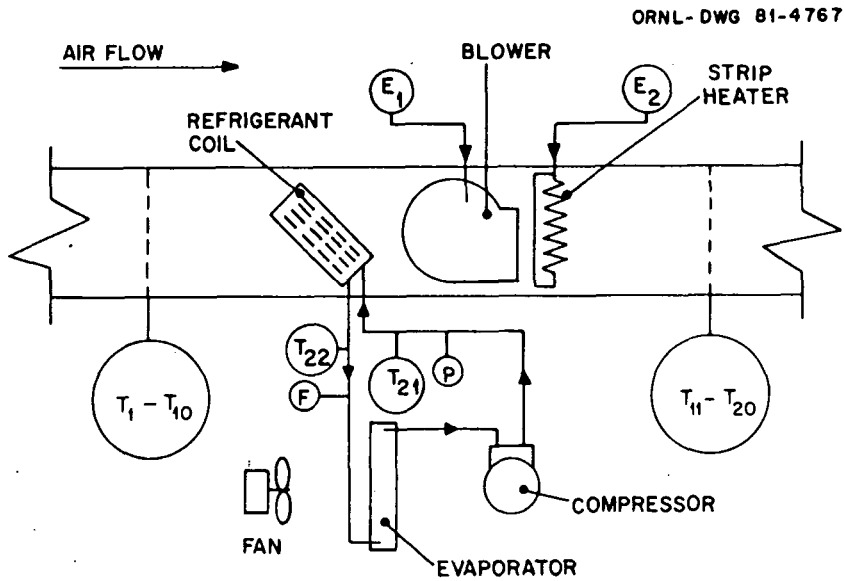

Point	Type*	Parameter	Sensor
E_1	1	Electrical power, indoor unit blower	Watthour meter
E_2	1	Electrical power, strip heaters	Watthour meter
F	0	Refrigerant flow rate	Turbine flow meter
T_1–T_{10}	0	Return air temperatures	Cu-Con thermocouples
T_{11}–T_{20}	0	Supply air temperatures	Cu-Con thermocouples
T_{21}	0	Refrigerant temperature entering indoor unit	Ch-Al thermocouple
T_{22}	0	Refrigerant temperature exiting indoor unit	Ch-Al thermocouple
P	1	Refrigerant pressure entering indoor unit	Bourdon tube gauge

*0 = data logged automatically on DAS, 1 = data logged manually in log book

Fig. 4.5. GE heat pump instrumentation.

locations at which the temperature and velocity measurements were made in the supply duct and the sensor location/description for this heat pump. A total of 45 tests were conducted with the GE heat pump, 22 in the resistance heating mode and 23 in the refrigerant heating mode. Software modifications to the DAS were necessary to accommodate the almost cyclic refrigerant flow variations caused by the thermostatic expansion valve; this cyclic flow did not occur in the Carrier unit because it uses a short tube expansion device rather than a valve to regulate the refrigerant flow. Two different schemes were used to deal with this cyclic refrigerant flow situation. One of these was to monitor continuously the refrigerant flowmeter and use this signal to trigger a DAS print/log operation when the signal dropped below a certain level. The average refrigerant flow rate since the previous print/log operation and the measured temperatures at

the time of the operation were thus logged as a data set. The second scheme was to scan all of the sensors once every 15 s and print/log the average of these measurements at 6-min intervals. Because the rate of cycling of the expansion valve was about once every 2.5 min, these 6-min intervals produced averages over at least two complete cycles. Refrigerant heat flow rate was calculated on the central computer systems at Oak Ridge National Laboratory using a computer subroutine rather than the interpolation/extrapolation method with the refrigerant tables. Referring to Fig. 4.4, points P, T_{21}, T_{22}, and F provided the necessary input data to the subroutine.

Switches in the circuit at the heat pump were used to power either two or three of the strip heater elements, giving two discrete power levels, which were used in the resistance heating tests. A conventional watt-hour meter was installed to measure the electrical power to the strip heaters. As the resistance heating tests could be run at steady state conditions, there was no need to use the refined DAS programs required for the refrigerant heating tests.

4.4 Assessment of Measurement System Error

Sensors and meters used to make the various measurements for this project were primarily those used by previous investigators. The DAS consists of a Digital Equipment Corporation PDP-8E computer and associated peripherals. Atypical duct systems, designed to provide fully developed turbulent flow, were used by these investigators so that heat balances could be performed around the indoor unit by measuring heat output on both the refrigerant side and the air side. Domingorena[3] reported a difference of 3% between the two methods in work with a Bard heat pump. Corrected data[4] from Domingorena's research with the Carrier heat pump[5] showed a difference of 5%, while Miller[6] reported a difference of <3% on the GE heat pump.

Because the heat flow measurements on the air side are more suspect than those on the refrigerant side, the bulk of these differences in the heat balance calculations are assumed to be errors in the air side method. Accuracy of the refrigerant side heat flow measurement is thus inferred to

be near 100% based on the work of these previous investigators. All of the analyses reported here were calculated assuming zero error in the measuring instruments.

5. CARRIER HEAT PUMP TESTING

The effects of fan speed, resistance heater power level, and distance of the supply air temperature sensors downstream from the indoor unit on the accuracy of the proposed heat flow measuring technique are summarized in Table 5.1. Magnitude of error at Position 1 is over twice that at Position 2 for both fan speeds and both heater power levels. Except for one data point, magnitude of error is considerably greater at the higher heater power level at both positions for both fan speeds. Only Positions 1 and 2 are used for the accuracy analysis because the absolute supply air temperatures at Position 3 were affected by ambient air mixing with the supply air in this region. Relative data concerning variation in velocity

Table 5.1. Effect of fan speed, resistance heater power level, and distance of supply air temperature sensors from indoor unit on accuracy of the proposed heat flow measuring technique for the Carrier test series

Position	Sensor distance from indoor unit (m)	Fan speed	Heater power level (kW)	Maximum error[a,b] (%)	Error of averages[b,c] (%)
1	0.23	Medium	2.42	−12.5	−11.5
1	0.23	Medium	4.42	−15.8	−14.3
1	0.23	High	2.55	−14.0	−8.6
1	0.23	High	4.54	−14.0	−11.2
2	0.56	Medium	2.39	+3.1	+0.2
2	0.56	Medium	4.34	+5.6	+2.9
2	0.56	High	2.51	+4.4	+2.1
2	0.56	High	4.49	+6.8	+4.0

[a]The maximum error is the error of worst case refrigerant K vs resistance K.

[b]The "−" sign indicates that the refrigerant heat flow is understated, and the "+" sign indicates that the refrigent heat flow is overstated.

[c]The error of averages is the error using average refrigerant K vs average resistance K.

and temperature is presented elsewhere for all three positions, however, because the mixing was not of sufficient magnitude to obscure the general trends. It is concluded from the data presented in Table 5.1 that the Carrier fan speed has only a small effect on the accuracy of the proposed technique, but the effects of resistance heater power level and temperature sensor distance downstream from the indoor unit are quite pronounced.

Velocity measurements made in the supply duct at the thermocouple locations and reduced velocity data are presented in Fig. 5.1. Standard deviation σ of each set of velocity measurements, used here as an index to magnitude of velocity variation, illustrates that distance down the supply duct from the indoor unit has a much greater effect on velocity variation than does fan speed. Degree of velocity variation decreases as distance from the indoor unit increases.

Supply duct temperature measurements and reduced temperature data for representative refrigerant heating tests are presented in Fig. 5.2, while Figs. 5.3 and 5.4 contain the same information for representative resistance heating tests at two heater power levels. Fan speed has an effect on temperature variation, for the standard deviation is generally somewhat higher for the medium fan speed than for the high fan speed for all three sets of data. These small differences are rather insignificant, however, when compared with the effects of distance from the indoor unit and heater power level on temperature variation. Standard deviation of the temperature measurements declines with increasing distance from the indoor unit for both refrigerant and resistance heating modes. For the resistance heating mode, standard deviation at Position 2 (0.56 m from indoor unit) is one-half that at Position 1 (0.23 m from indoor unit) for both fan speeds and both heater power levels. Standard deviation also differs by a factor of 2 for the low power level vs the high power level at all three positions for both fan speeds. Temperature variation across the supply duct in the resistance heating mode is thus shown to decrease as (1) temperature sensor distance from the indoor unit increases and (2) resistance heater power level decreases.

ORNL-DWG 81-4774

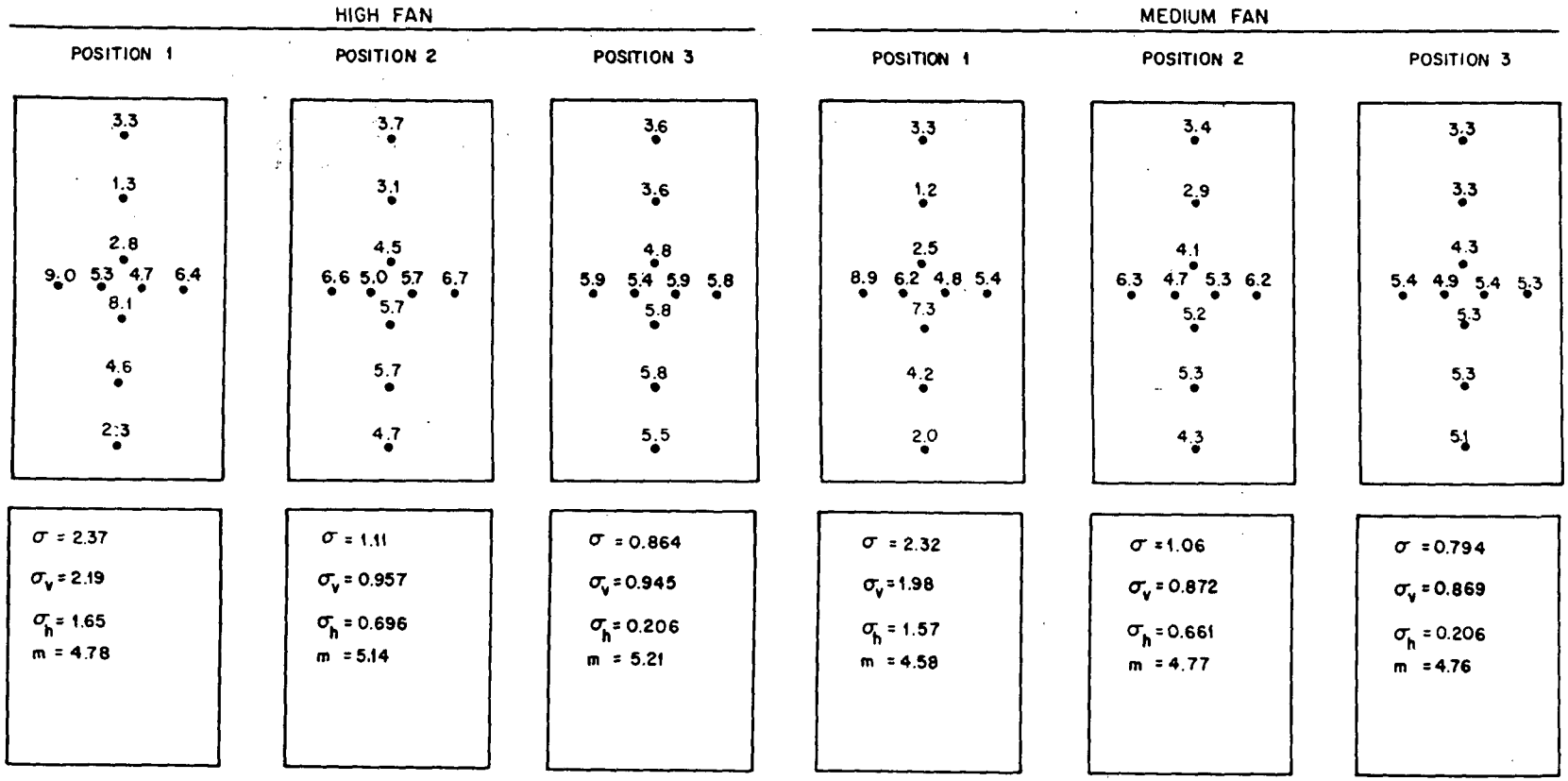

σ = STANDARD DEVIATION OF ALL 10 MEASUREMENTS

σ_v = STANDARD DEVIATION OF ALL MEASUREMENTS ON VERTICAL LINES

σ_h = STANDARD DEVIATION OF ALL MEASUREMENTS ON HORIZONTAL LINES

m = MEAN SUPPLY AIR VELOCITY

Fig. 5.1. Carrier supply duct air velocity data. Air velocity units are meters per second.

ORNL-DWG 81-4773

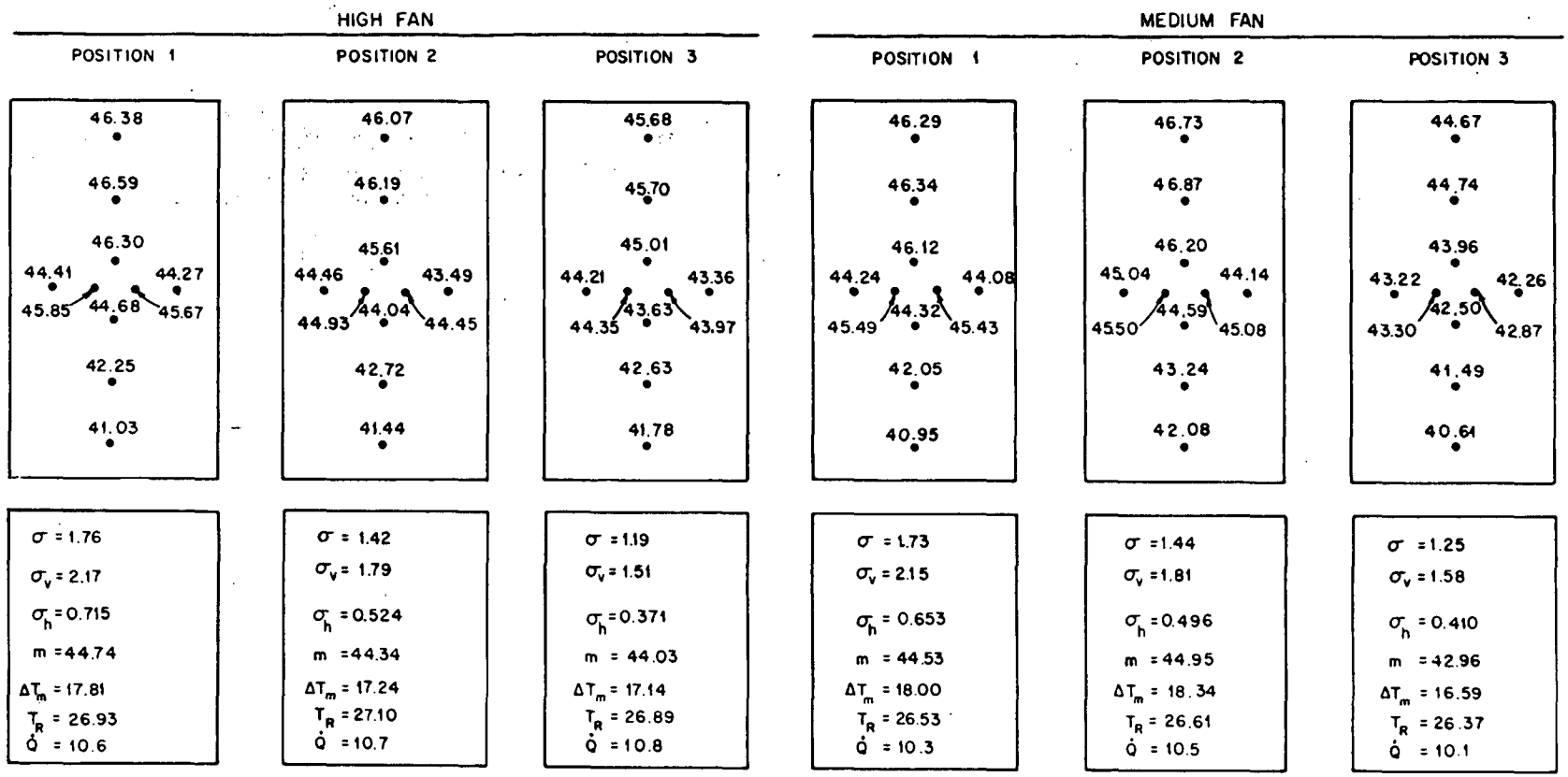

σ = STANDARD DEVIATION OF ALL 10 MEASUREMENTS

σ_v = STANDARD DEVIATION OF ALL MEASUREMENTS ON VERTICAL LINES

σ_h = STANDARD DEVIATION OF ALL MEASUREMENTS ON HORIZONTAL LINES

m = MEAN SUPPLY AIR TEMPERATURE

ΔT_m = MEAN TEMPERATURE DIFFERENCE

T_R = MEAN RETURN AIR TEMPERATURE

$\dot{Q}$ = HEAT FLOW RATE

Fig. 5.2. Carrier supply duct air temperature data, refrigerant heating mode. Temperature units are degrees Celsius, and heat flow rate units are kilowatts.

ORNL-DWG 81-4775

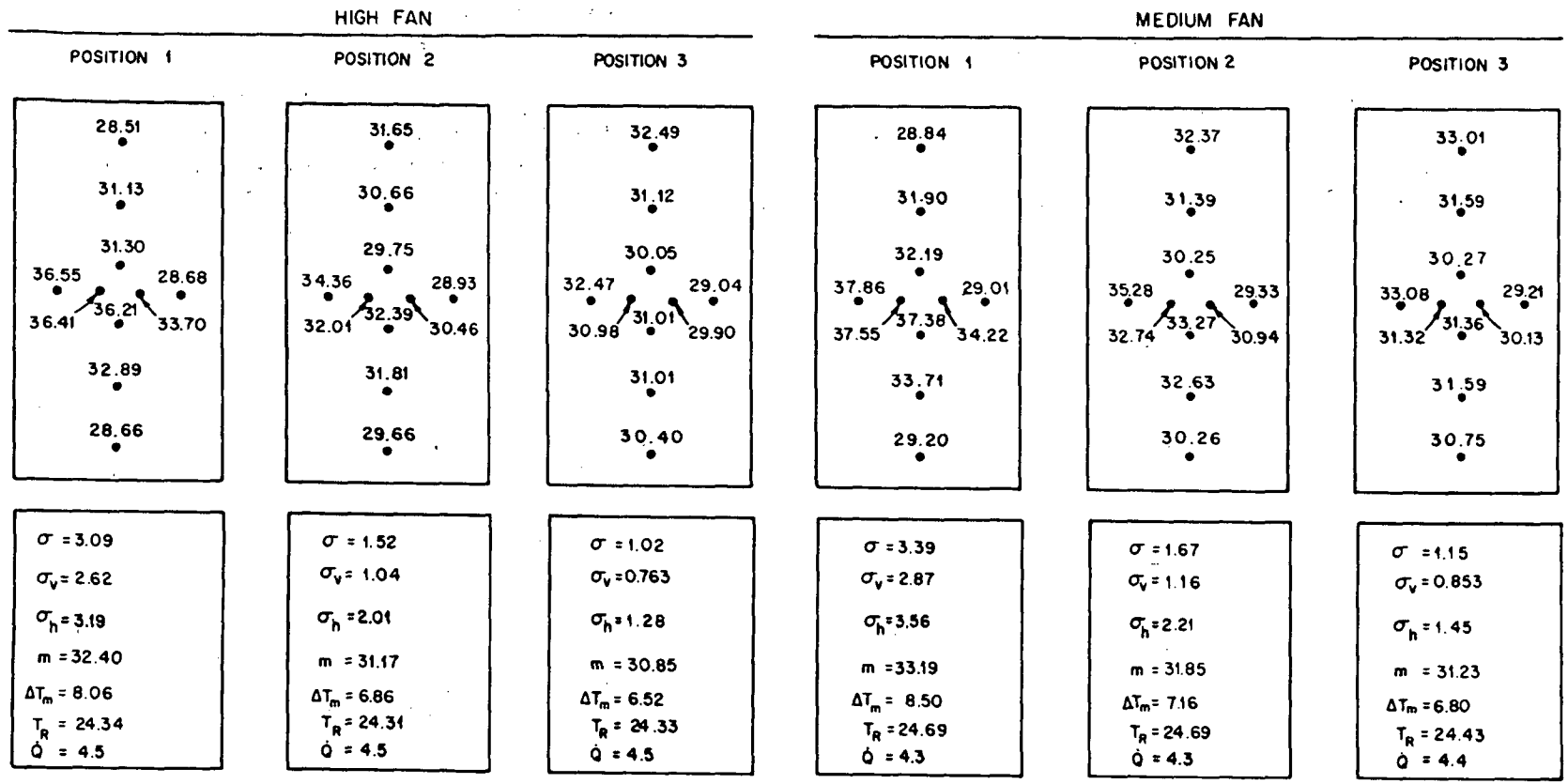

σ = STANDARD DEVIATION OF ALL 10 MEASUREMENTS

σ_v = STANDARD DEVIATION OF ALL MEASUREMENTS ON VERTICAL LINES

σ_h = STANDARD DEVIATION OF ALL MEASUREMENTS ON HORIZONTAL LINES

m = MEAN SUPPLY AIR TEMPERATURE

ΔT_m = MEAN TEMPERATURE DIFFERENCE

T_R = MEAN RETURN AIR TEMPERATURE

$\dot{Q}$ = HEAT FLOW RATE

Fig. 5.3. Carrier supply duct air temperature data, resistance heating mode – high heater power level. Temperature units are degrees Celsuis, and heat flow rate units are kilowatts.

ORNL-DWG 81-4776

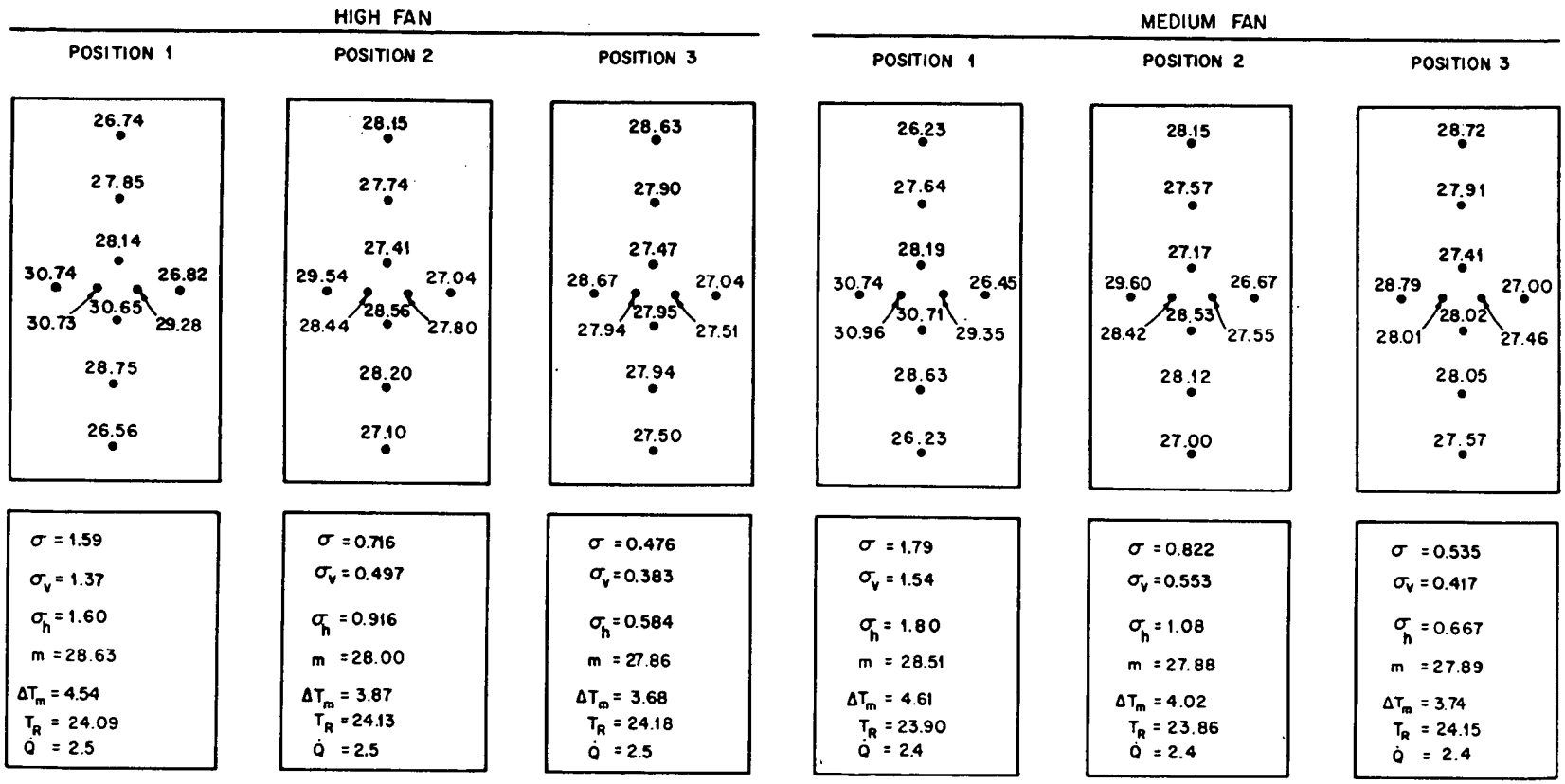

Fig. 5.4. Carrier supply duct air temperature data, resistance heating mode – low heater power level. Temperature units are degrees Celsuis, and heat flow rate units are kilowatts.

6. GE HEAT PUMP TESTING

A summary of the accuracy analysis for the GE test series is presented in Table 6.1. At Position 1, the error for the higher resistance heater power level is over twice that for the lower power level. For the lower power level, the error at Position 1 is only one-half that at Position 2. Only Positions 1 and 2 were used for this analysis because the supply air temperature at Position 3 (near the duct exit) was affected by ambient air mixing in this region.

As fan speed on the Carrier unit had a negligible effect on the accuracy of the proposed heat flow measuring technique, all of the tests on the GE unit were conducted at a single fan speed. Supply duct air velocity measurements were made on the GE system with the same instruments and procedures that were used on the Carrier system. These velocity measurements and reduced velocity data are reported in Fig. 6.1. Also shown in this figure are air temperature measurements and reduced temperature data for representative refrigerant heating tests, while Fig. 6.2 presents

Table 6.1. Effect of resistance heater power level and distance of supply air temperature sensors from indoor unit on accuracy of the proposed heat flow measuring technique for the GE test series

Position	Sensor distance from indoor unit (m)	Heater power level (kW)	Maximum error[a,b] (%)	Error of averages[b,c] (%)
1	0.89	9.69	−2.8	−1.2
1	0.89	15.68	−7.4	−5.6
2	1.22 + transition	9.70	+5.6	+2.2
2	1.22 + transition	15.66	+6.7	+3.2

[a]The maximum error is the error of worst case refrigerant K vs resistance K.

[b]The "−" sign indicates that the refrigerant heat flow is understated, and the "+" sign indicates that the refrigerant heat flow is overstated.

[c]The error of averages is the error using average refrigerant K vs average resistance K.

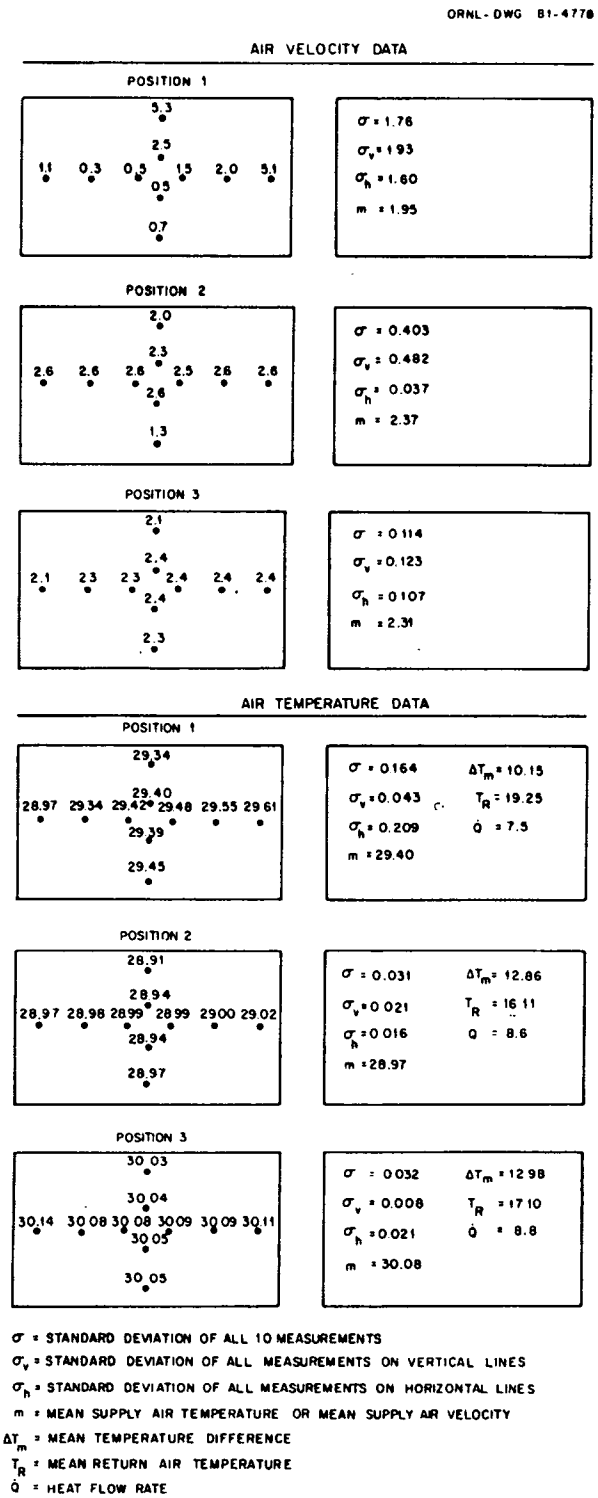

Fig. 6.1. GE supply duct air velocity data and refrigerant heating mode air temperature data — high fan speed. Air velocity units are in meters per second, temperature units are in degrees Celsius, and heat flow rate units are in kilowatts.

ORNL-DWG 81-4777

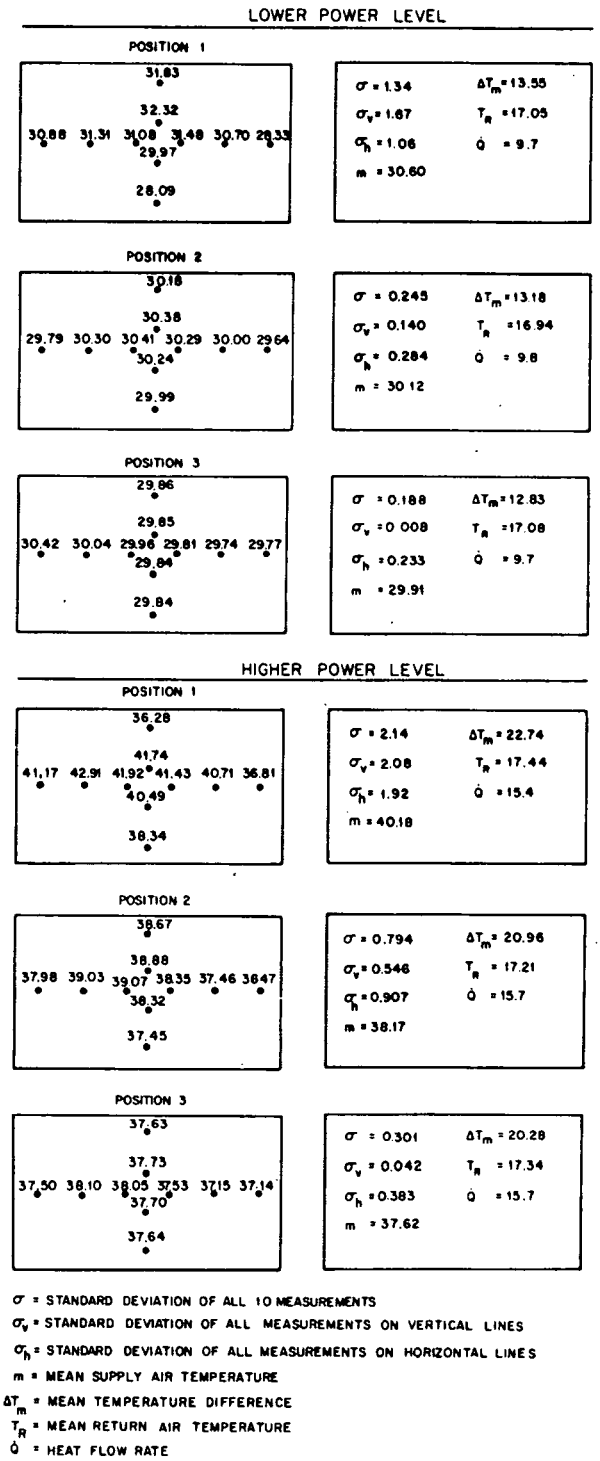

Fig. 6.2. GE supply duct air temperature data, resistance heating mode — high fan speed. Temperature units are in degrees Celsius, and heat flow rate units are in kilowatts.

similar data for representative resistance heating tests. General trends observed in the Carrier test data are also shown here. Both velocity variation and temperature variation decrease as distance from the indoor unit increases. At any of the three duct cross sections, temperature variation in the resistance heating mode is much less at the lower power level than at the higher power level. Supply air temperature variation in the refrigerant heating mode is considerably less than that in the resistance heating mode.

7. EVALUATION OF TEST DATA

Similarities and differences between the two heat pump systems should be noted before the results of the tests on both units are considered together. Mean supply air velocity for the Carrier at the high fan speed is twice that of the GE system at the high fan speed. Air mass flow rate through the two systems was not drastically different, however; the Carrier flow rate at the high fan speed was nine-tenths that of the GE at the high fan speed, while the Carrier flow rate at the medium fan speed was eight-tenths that of the GE at the high fan speed. Differences in duct cross-sectional area and air density at the time of testing account for most of the differences in mean velocities.

That the two systems are geometrically similar can be seen from Figs. 7.1 and 7.2. These photographs of the downstream ends of the Carrier and GE indoor units, respectively, were shot from a point downstream in the supply air duct. While the cross-sectional area of the Carrier duct is about one-half that of the GE, the general arrangement of blower discharge and duct height to width ratio are much the same for the two systems. GE duct cross-sectional area to blower discharge area is nearly twice that of the Carrier, however.

Velocity and temperature data for both heat pumps are summarized in Table 7.1. Standard deviation of the velocity measurements shows the velocity variation to be greater for the GE than for the Carrier at the same distance down the supply duct from the indoor unit, which is Carrier Position 3 and GE Position 1. Velocity variation relative to mean velocity is even more pronounced, the ratio of standard deviation to mean velocity for the GE being more than five times that of the Carrier. Heat flow measurement, however, is directly a function of mass flow rate and only indirectly a function of velocity; because the air mass flow rate for the two systems was about the same, standard deviation of the velocity measurements in the supply duct is a more valid indicator of mass flow variation than the ratio of standard deviation to mean velocity.

ORNL-PHOTO 7073-80

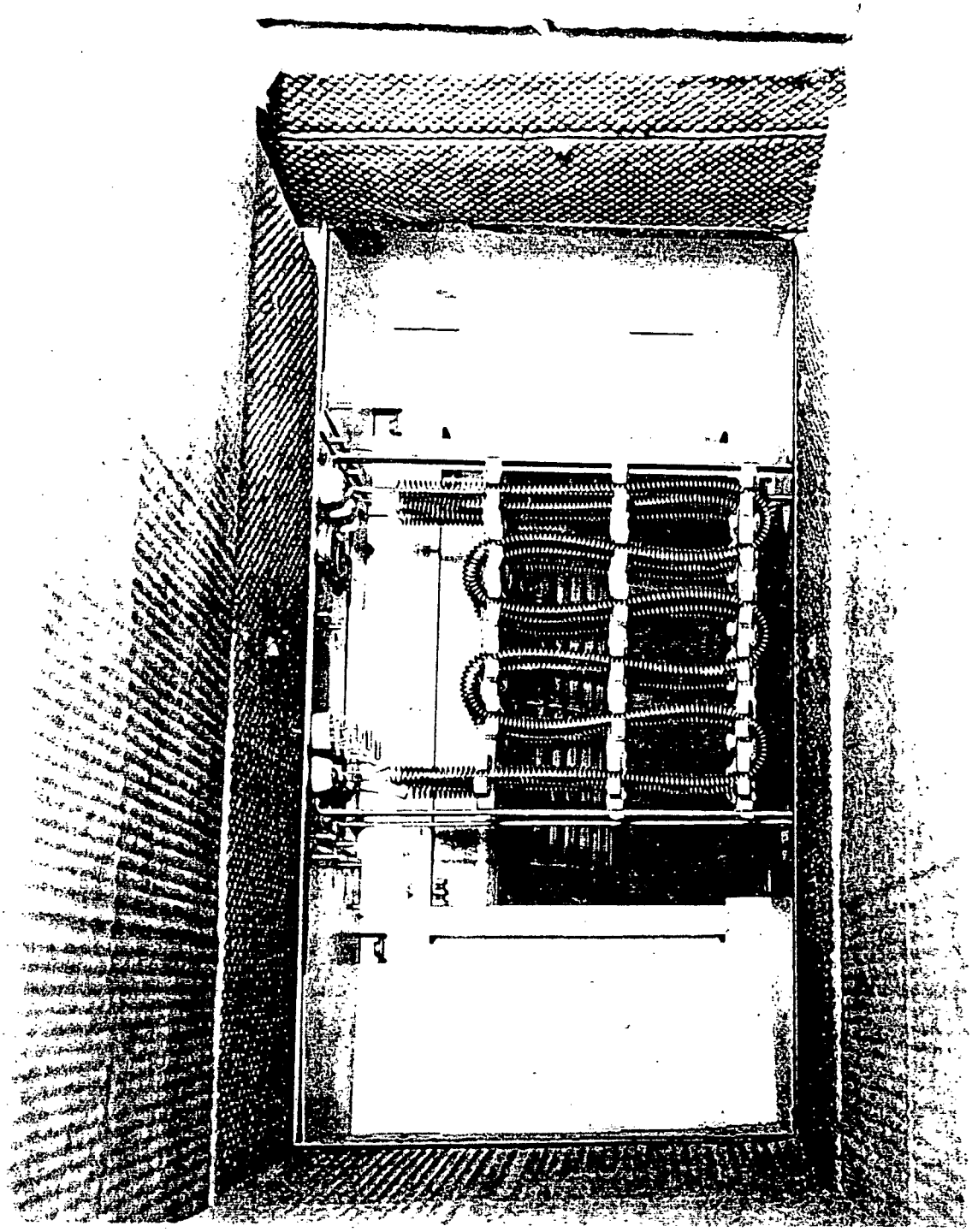

Fig. 7.1. Carrier indoor unit and supply duct viewed from a point downstream in the supply duct.

ORNL–PHOTO 7017–81

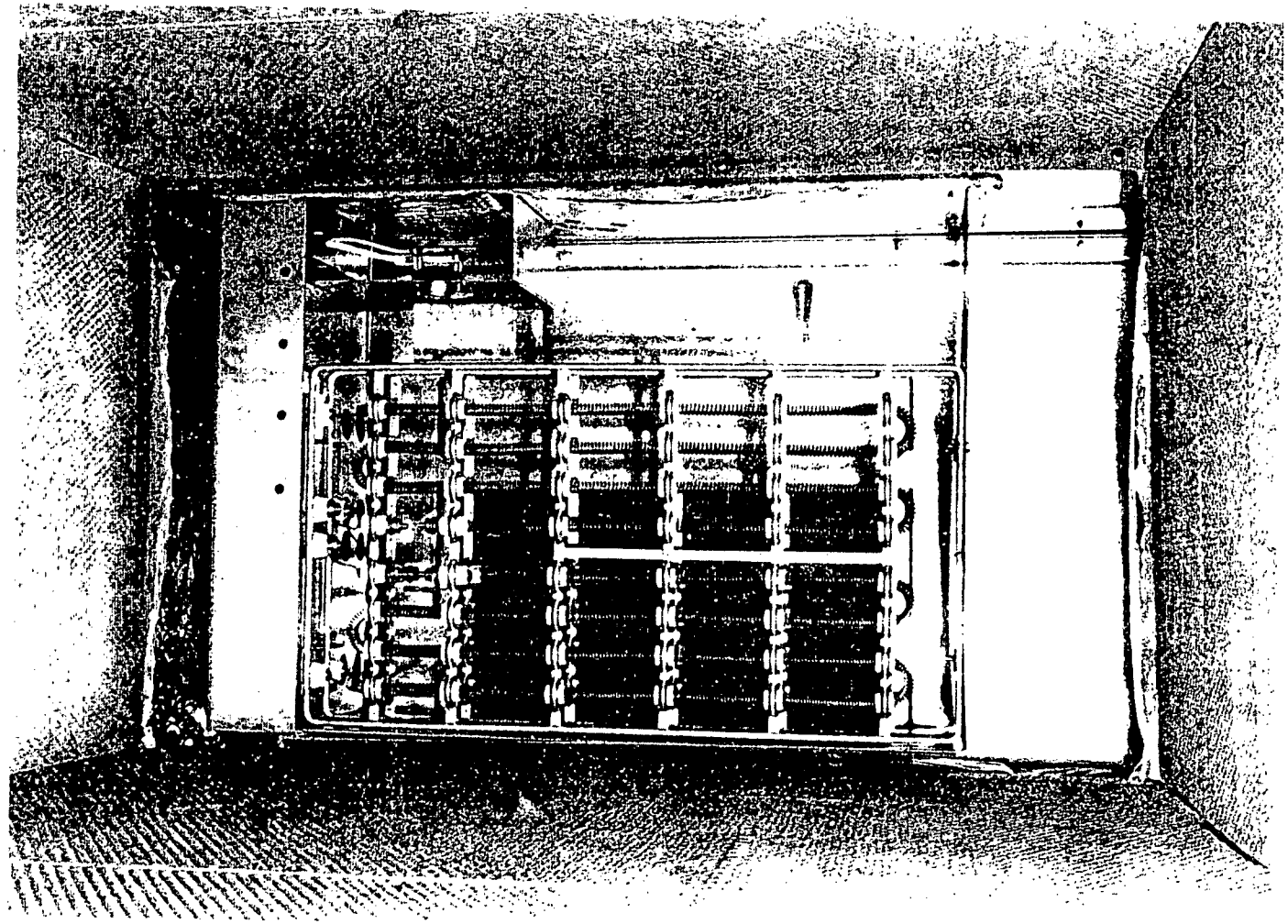

Fig. 7.2. GE indoor unit and supply duct viewed from a point downstream in the supply duct.

Table 7.1. Summary of supply air velocity and temperature data

Heat pump and grid position	Fan speed	Sensor distance from indoor unit (m)	Velocity data		Refrigerant heating mode supply air temperature data[a]			Resistance heating mode supply air temperature data					
								Lower power level[a]			High power level[a]		
			Standard deviation	Mean velocity (m/s)	Standard deviation	ΔT_m (°C)	$\dot{Q}$ (kW)	Standard deviation	ΔT_m (°C)	$\dot{Q}$ (kW)	Standard deviation	ΔT_m (°C)	$\dot{Q}$ (kW)
C-1	Medium	0.23	2.32	4.58	1.73	18.00	10.3	1.79	4.61	2.4	3.39	8.50	4.3
C-1	High	0.23	2.37	4.78	1.76	17.81	10.6	1.59	4.54	2.5	3.09	8.06	4.5
C-2	Medium	0.56	1.06	4.77	1.44	18.34	10.5	0.822	4.02	2.4	1.67	7.16	4.3
C-2	High	0.56	1.11	5.14	1.42	17.24	10.7	0.716	3.87	2.5	1.52	6.86	4.5
C-3	Medium	0.89	0.794	4.76	1.25	16.59	10.1	0.535	3.74	2.4	1.15	6.80	4.3
C-3	High	0.89	0.864	5.21	1.19	17.14	10.8	0.476	3.68	2.5	1.02	6.52	4.5
G-1	High	0.89	1.76	1.95	0.164	10.15	7.0	1.34	13.55	9.7	2.14	22.74	15.4
G-2	High	1.22 + transition	0.403	2.37	0.031	12.86	8.6	0.245	13.18	9.8	0.794	20.96	15.7
G-3	High	3.05 + transition	0.114	2.31	0.032	12.98	8.8	0.188	12.83	9.7	0.301	20.28	15.7

[a] ΔT_m is the mean temperature difference between supply air and return air, and $\dot{Q}$ is the heat added to air stream.

7.1 Normalized Temperature Difference Variation

In an effort to quantify the relationship between resistance heater power level and supply air temperature variation, a method of normalizing the experimental data was needed. The method chosen here was to use the ratio of supply air temperature measurement standard deviation to average temperature difference between return and supply air streams. Units of this ratio are therefore standard deviation per degree Celsius mean temperature difference. Normalized temperature difference variation for both heat pumps is presented in Table 7.2. Temperature difference variation in the refrigerant heating mode is much less for the GE than for the Carrier, and in both heat pumps the variation in the refrigerant heating mode is less than in the resistance heating mode. Data from both heat pumps do not support the hypothesis that higher power levels cause greater temperature difference variation on a per unit basis. The observed accuracy vs power level phenomenon is therefore inferred to be caused by the interaction of the velocity and temperature difference profiles in such a way as to make the error proportional to magnitude of temperature difference variation rather than variation per unit of temperature difference.

Table 7.2. Normalized temperature difference variation (standard deviation/mean temperature difference) for both test series

Heat pump	Heating mode	Position 1	Position 2	Position 3	Fan speed
Carrier	Resistance, low power	0.388	0.204	0.143	Medium
Carrier	Resistance, high power	0.399	0.233	0.169	Medium
Carrier	Refrigerant	0.096	0.079	0.075	Medium
Carrier	Resistance, low power	0.350	0.185	0.129	High
Carrier	Resistance, high power	0.383	0.222	0.156	High
Carrier	Refrigerant	0.099	0.082	0.069	High
GE	Resistance, low power	0.099	0.019	0.015	High
GE	Resistance, high power	0.094	0.038	0.015	High
GE	Refrigerant	0.016	0.002	0.002	High

7.2 Effect of Temperature Sensor Configuration on Accuracy

The type of temperature sensors chosen for a COP meter would have a significant impact on cost and simplicity of operation. The suitability of three generic types of sensors for use in such a meter was examined:

1. point sensors — to measure the temperature at a single point,
2. line averaging sensors — to measure the average temperature along a straight line, and
3. area sensors — to measure the average temperature over some area.

Because there was negligible temperature variation in return air at the return thermocouple grid, the average of these temperature measurements was used for return air temperature for all analyses. Point sensor performance was determined by using the four temperature measurements made nearest the center of the supply duct and the average return air temperature to calculate four sets of ΔTs. These analyses are reported in Table 7.3 as point error. Line averaging sensor performance was determined by using the average of the temperature measurements along the horizontal and vertical lines passing through the center of the supply duct and the average return air temperature to calculate two sets of ΔTs. These analyses are reported in Table 7.3 as horizontal error and vertical error, respectively. Area sensor performance was determined by using the average temperature measured over both the horizontal and the vertical lines passing through the center of the supply duct and the average return air temperature to calculate a single ΔT for each test. These analyses are reported in Table 7.3 as grid error and constitute the same data as previous accuracy analyses.

Examination of the point error data confirms what one would suspect to be the case where both velocity and temperature are nonuniform — degree and direction of error are so unpredictable as to make the use of point temperature sensors quite unsuitable for precision work. The GE Position 2 data is quite good, but a convenient explanation for this based on scientific principles is not apparent.

An interesting fact comes to light when the horizontal and vertical data are compared with the grid data. The GE vertical errors are less

Table 7.3. Error analysis of the proposed heat flow measuring technique based on the parametric investigation conducted in the laboratory

Heat pump and grid position	Fan speed	Sensor distance from indoor unit (m)	Heater power (kW)	Grid error[a]		Horizontal error[a]		Vertical error[a]		Point error – maximum[a,b] (%)			
				Maximum error[b] (%)	Error of averages[c] (%)	Maximum error[b] (%)	Error of averages[c] (%)	Maximum error[b] (%)	Error of averages[c] (%)	Point 1	Point 2	Point 3	Point 4
C-1	Medium	0.23	2.42	-12.5	-11.5	-22.7	-21.1	-0.7	+1.1	-41.1	+5.1	-21.6	-39.2
C-1	Medium	0.23	4.42	-15.8	-14.3	-24.8	-23.6	-3.9	-2.0	-42.3	+10.3	-20.7	-39.7
C-1	High	0.23	2.55	-14.0	-8.6	-22.9	-17.9	+9.8	+3.5	-40.5	+14.2	-19.8	-36.7
C-1	High	0.23	4.54	-14.0	-11.2	-23.2	-20.6	+4.3	+1.3	-41.4	+18.1	-20.9	-38.2
C-2	Medium	0.56	2.39	+3.1	+0.2	-4.9	-3.4	+8.1	+4.1	-14.5	+44.3	+25.9	-8.2
C-2	Medium	0.56	4.34	+5.6	+2.9	-3.2	-0.2	+10.7	+6.4	-17.6	+50.7	+25.4	-8.0
C-2	High	0.56	2.51	+4.4	+2.1	-3.7	-1.9	+9.2	+6.4	-12.6	+53.1	+27.9	+5.8
C-2	High	0.56	4.49	+6.8	+4.0	-1.6	0.0	+12.5	+8.4	-14.9	+54.5	+26.0	-6.0
G-1	High	0.89	9.69	-2.8	-1.2	-3.1	-1.6	-2.6	-0.8	-7.9	-7.2	+5.5	-14.3
G-1	High	0.89	15.68	-7.4	-5.6	-10.6	-9.0	-4.1	-1.9	-12.2	-14.4	-9.6	-13.7
G-2	High	1.22 + transition	9.70	+5.6	+2.2	+6.4	+3.3	+4.8	+1.1	+4.7	-2.2	+4.7	+3.4
G-2	High	1.22 + transition	15.66	+6.7	+3.2	+7.3	+4.2	+6.1	+2.1	+6.5	-2.8	+6.3	+3.4

[a]The "–" sign indicates that the refrigerant heat flow is understated, and the "+" sign indicates that the refrigerant heat flow is overstated.

[b]The maximum error is the error of worst case refrigerant K vs resistance K.

[c]The error of averages is the error using average refrigerant K vs average resistance K.

than GE grid errors for all four conditions, and Carrier horizontal errors are less than Carrier grid errors for three of the four conditions at Position 2. GE vertical and Carrier horizontal correspond to lines that (1) span the short dimension of the duct, and (2) pass through the center of the duct perpendicular to the duct wall and to the blower axis. While examination of the velocity and temperature data presented does not strongly support the hypothesis that a line averaging sensor used in the manner described in the preceding paragraphs would be acceptable for COP tests on installed units, the hypothesis is an attractive one because it would reduce the first cost and simplify the use of a COP meter.

7.3 Error Direction

Direction of error is caused by a combination of two factors:

1. shape of velocity and temperature difference profiles, and
2. radiative biasing of the supply air temperature sensors.

Dissimilar temperature difference profiles exist for the two heating modes in both heat pump systems. Error direction could then be either positive or negative depending upon the combination of velocity and temperature difference profiles for both heating modes. Radiative biasing would cause errors to be in the negative direction with the sign conventions here adopted and would have a greater effect at the position nearer the indoor unit and at the higher heater power levels. Uneven air flow over the resistance heating elements allowed portions of the elements to become incandescent during many of the tests, so radiative biasing probably occurred to some degree.

7.4 Estimated Accuracy in Field Applications

For the laboratory experiments, magnitude of heat flow measurement error was generally less at the:

1. greater distance of the supply air temperature sensor from the indoor unit, and
2. lower resistance heater power level.

Because differing temperature profiles are found in the supply duct for resistance heating and refrigerant heating, increased errors can occur if the supply air temperature sensor is installed downstream of any supply duct branching. Figure 7.3 illustrates this situation. Even though mass flow rate and system heat flow rate are the same for both heating modes in this example, the ratio of heat flow to temperature difference is not the same for either duct A or duct B for both heating modes. Accuracy of the proposed heat flow measuring technique under these conditions cannot be estimated from information presently available. Heat pump dealers and refrigeration engineers consulted about heat pump duct systems stated that most systems would have at least 1.5 to 2 m of supply duct before branching. One large distributor estimated that <10% of the systems in use today would have <1 m before branching.

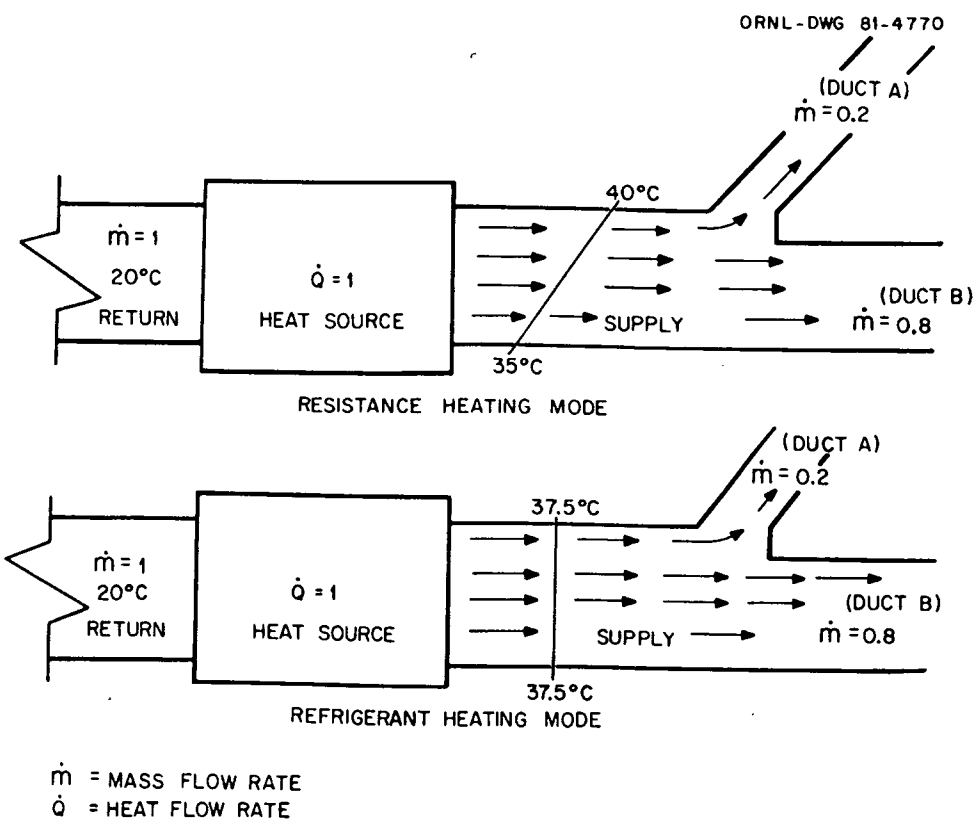

Fig. 7.3. Effect of dissimilar temperature profiles for resistance and refrigerant heating modes on heat flow in branch ducts.

From these industry contacts, it is assumed that a minimum distance of 1 m from indoor unit to supply air temperature sensor will be available for at least 90% of the residential heat pump systems now in use. Thus, the Carrier Position 2 data and the GE Position 1 data are taken to be conservatively representative of 90% of the units operating today. Based on these data and the observed relationship between error and resistance heater power level, accuracy of the proposed heat flow measuring technique on field units is estimated to be within 5% provided that:

1. supply air temperature sensors are area type sensors and are located at least 1 m downstream of the indoor unit, and
2. indoor unit strip heaters used for the calibration process are limited to a power level of 5 kW or less.

8. RECOMMENDATIONS

The proposed heat flow measuring technique appears to be a feasible means of measuring heat flow in installed heat pumps. A prototype COP meter, such as that described in the appendix, should be built to check the accuracy of the proposed technique on other heat pump systems that are sufficiently instrumented to provide independent verfication of the COP meter operation. These heat pump systems can be found at many of the research facilities throughout the country where heat pump research is conducted.

Two items especially merit further investigation:

1. Resistance heaters used for calibration. If a low wattage unit, perhaps 1 to 3 kW, were placed in the return air duct close to the indoor unit, the supply air temperature variation should be considerably less than when using the heat pump strip heaters. Heated air from the heater would travel through both the refrigerant coil and the blower before entering the supply duct; this opportunity for mixing could well produce a supply air temperature as uniform as that observed for refrigerant heating. Errors using this arrangement might well be less than half those observed in the laboratory using the strip heaters.

2. Type of temperature sensor. If a fairly uniform temperature difference between return and supply air can be attained by the method described in the preceding paragraphs, line averaging sensors could be used instead of area sensors. This would simplify sensor installation on a unit and reduce the first cost of the total instrument package.

REFERENCES

1. American Society of Heating, Refrigerating, and Air-Conditioning Engineers, *Methods of Testing for Rating Unitary Air Conditioning and Heat Pump Equipment*, ASHRAE Standard 37-69 (April 1969).

2. American National Standards Institute, *American National Standards Performance Requirements for Oil-Powered Central Furnaces*, ANSI Z91.1-1972 (June 1972).

3. A. A. Domingorena, *Performance Evaluation of a Low-First-Cost, Three-Ton, Air-to-Air Heat Pump in the Heating Mode*, ORNL/CON-18 (October 1978).

4. C. K. Rice, Oak Ridge National Laboratory, private communication.

5. A. A. Domingorena and S. J. Ball, *Performance Evaluation of a Selected Three-Ton Air-to-Air Heat Pump in the Heating Mode*, ORNL/CON-34 (January 1980).

6. W. A. Miller and S. J. Ball, *Performance Evaluation at Various Ambient Relative Humidities of a High-Efficiency Air-to-Air Heat Pump in the Heating Mode* (working title), ORNL/CON-69 (in preparation).

7. W. H. Andrews, *An Optical Watthour Meter Digitizer*, ORNL/TM-7355 (October 1980).

Appendix*

COP METER — THEORY OF OPERATION AND PROTOTYPE DESIGN

The COP Meter is a device that permits efficiency measurements on installed heat pumps in a matter of minutes. Coefficient of performance (COP) is a dimensionless number used to characterize the performance of heat pumps. The definition of COP for a heat pump in the heating mode is

$$COP = \dot{Q}/P ,$$

where $\dot{Q}$ is the heat output of the indoor unit and P is the power input to the heat pump. A variety of instruments are available to measure electrical power input, but heat flow is not as amenable to direct measurement as electrical power. The theory of operation of the COP Meter's heat flow measuring technique is derived from the first law of thermodynamics. The first law for a steady-state, steady-flow system where no work is done may be written

$$\dot{Q} = \dot{m}\, C_p\, \Delta T ,$$

where

$\dot{Q}$ = heat flow rate,

$\dot{m}$ = mass flow rate of the heat transfer fluid,

C_p = specific heat of the fluid at constant pressure, and

ΔT = temperature difference between the entering and exiting fluid streams.

If the mass flow rate and the specific heat are constant, this equation reduces to $\dot{Q} = K\Delta T$. The COP Meter is calibrated in place for each heat pump to be tested. This is done by running the heat pump in the resistance heating mode to determine the relationship of heat flow to temperature difference for that particular system. This relationship is then

*Material excerpted from patent disclosure information submitted to the Department of Energy Patent Office — patent pending to coinventors V. R. Brantley and D. R. Miller.

used to calculate the heat flow when the heat pump is operated in the normal refrigerant heating mode from the measured temperature difference at that time.

The operating procedure requires no specialized knowledge of either electronics or thermodynamics. With the temperature sensors placed in the return and supply air ducts and the power measuring leads connected in the heat pump electrical supply circuit, the heat pump is run in the normal refrigerant heating mode. After ~10 min continuous operation for stabilization, the trim potentiometer in the amplifier gain circuit (pin 14, AD522) is adjusted until the E_{out} (pin 7, AD522) voltage is about 8.0 V. This optimizes the circuitry for the particular heating system being tested. The heat pump is switched to the resistance heating mode, and the calculator is initialized by zeroing the display and keying "+1" on the keyboard. This has set the calculator's counting increment to 1.0; for every pulse except the first to the calculator from the "and" gate and the divider, the displayed number will be incremented by 1.0. After at least 10 min has elapsed since the switch to the resistance heating mode, the "run" switch (pin 5, 4001) is depressed. The calculator will now up-count in increments of 1.0 for several minutes; the "run" cycle will have terminated when the calculator ceases to up-count. Because the COP of a heat pump operating in the resistance heating mode is 1.00, the reciprocal of the number displayed is the correct counting increment for this particular test series. Adequate accuracy and resolution is given if the reciprocal is rounded off to the same number of significant digits as the number from which it is derived.

After switching the heat pump to the normal refrigerant heating mode, the calculator is initialized by zeroing the display and keying "+ (reciprocal)" on the keyboard. When the system has had sufficient time to equilibrate (10 min or more), the "run" switch is depressed. The calculator now up-counts using the increment entered; at the termination of the "run" cycle, the number shown on the calculator display is the integrated COP of the heat pump over the whole "run" cycle.

Figure A.1 is a general flow sheet, and Fig. A.2 is a design schematic for a prototype COP Meter. Circuit changes and component substitutions can be made to improve the performance or to reduce the cost of

ORNL-DWG 81-4769

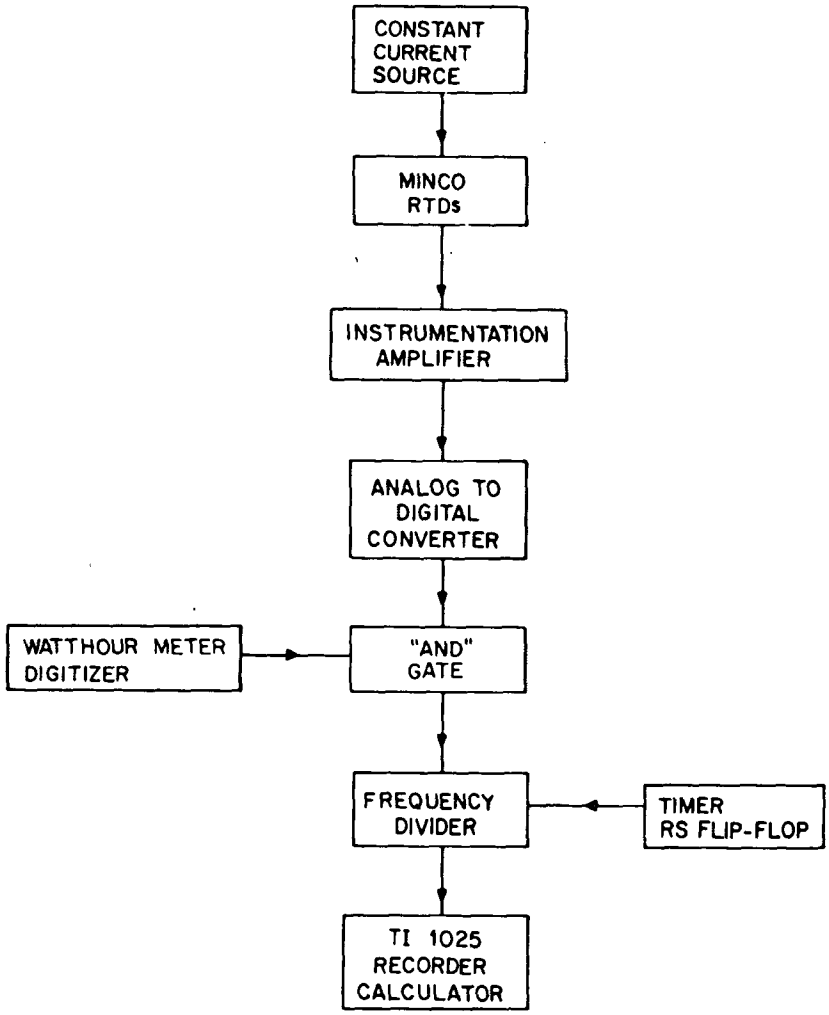

Fig. A.1. COP meter flow schematic.

the instrument, but these modifications will not affect the basic characteristics of the COP Meter. These basic characteristics are:

1. The COP Meter is a portable device that measures both heat flow and electrical power consumption and establishes a ratio for these measurements in such a way as to give a single number at the end of a test that represents the integrated COP of a heat pump over the test interval.

2. The COP Meter makes use of a resistance heating element to calibrate the device in place for each heating system to be tested, thus making it possible to test systems having quite different air flow rates and temperature differences with a single instrument.

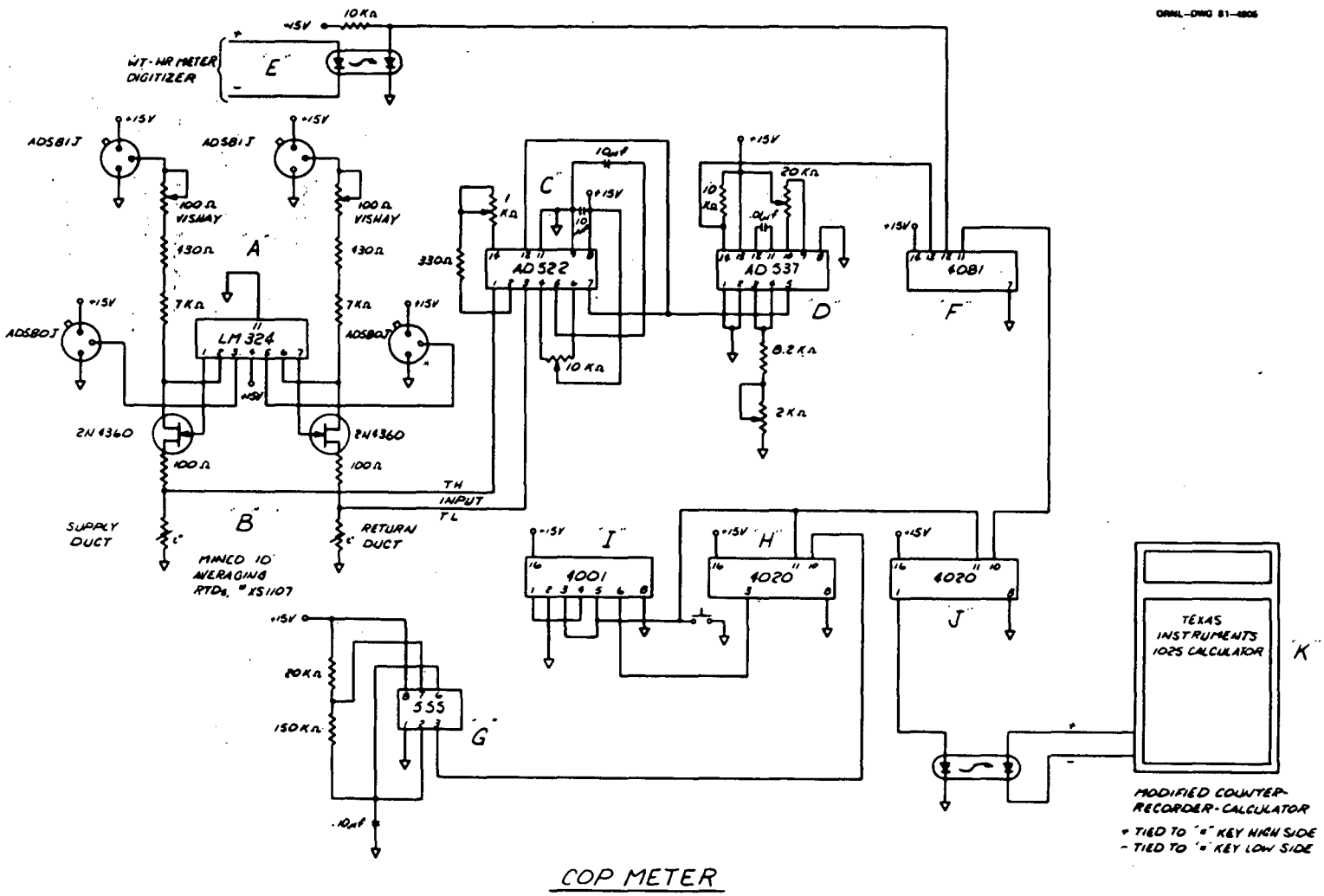

Fig. A.2. Prototype COP meter circuit design.

The prototype design uses (A) two constant current sources to supply 1 mA current each to (B) two Resistance Temperature Detectors (RTDs). These sensors have identical resistance/temperature characteristics so that the temperature difference between them can be accurately known over a range of temperatures by measuring the differential EMF generated by the constant current through them. This EMF is amplified by (C) a variable gain instrumentation amplifier whose output is a positive dc voltage linearly proportional to the EMF input. The amplifier output is routed to (D) an analog-to-digital converter whose output is a square wave. The frequency of this signal is linearly proportional to the input voltage. The output of the converter is connected to one input of (F) an "and" gate; the state of the other "and" gate input is controlled by (E) the Watthour Meter Digitizer via an optical isolator. The Watthour Meter Digitizer was developed at Oak Ridge National Laboratory (ORNL) and is completely described by W. H. Andrews.[7] Signal output of the Watthour Meter Digitizer is a positive pulse of fixed duration, and frequency of this pulse is linearly proportional to the heat pump electrical power input. A pull-up resistor is used to hold the "and" gate input high. This input is pulled low by the optical isolator for each positive pulse from the Watthour Meter Digitizer. For a given ΔT and its corresponding frequency from the analog-to-digital converter, less electrical power to the heat pump means a higher COP. Thus, the "and" gate on-time is greater for lower power input and less for higher power input.

Square wave signals from the "and" gate go to a divider chip that can be zeroed and its output held low by (I) a set-reset flip flop. Output state of the flip flop is determined by the manually operated run switch and (H) the timer signal divider. The state of the set input of the flip flop is controlled by a timer circuit using (G) a 555 astable multivibrator and (H) a signal divider. This divider output is normally low, but goes high after 16,384 pulses from the multivibrator. Design frequency of the multivibrator is 45 Hz, so the time necessary for the divider to go from a zeroed low output state to a high output state is 16,384/45 = 364 s or about 6 min. Digital logic provides the repeatability of this timer necessary for COP Meter accuracy. Absolute time interval is not critical but must be of sufficient length to ensure adequate

data input for a test. When the flip flop is in its "run" state, the divider downstream of the "and" gate is also operative. The output of this divider causes (K) the Texas Instruments calculator to increment the number in its display by the programmed amount. Output/input ratio for this divider is 1:4096; for every 4096 pulses through the "and" gate, the divider output goes high and causes the calculator to increment the displayed number by the programmed amount.

Three major modifications can be made in the COP Meter to increase its utility as a mechanic's troubleshooting tool or as a researcher's monitoring instrument. These are modifications that would enable the COP Meter to:

1. measure cooling COP as well as heating COP,
2. measure air flow rate, and
3. continuously record heat flow from any central forced-air distribution heating system.

For cooling COP, dry bulb temperature of the entering and exiting air streams is inadequate to calculate the heat removed from the air. This is due to moisture removal during air-conditioning, and this latent heat removal is not indicated by dry bulb temperature. The appropriate equation for this condition is

$$\dot{Q} = \dot{m}\Delta h ,$$

where Δh is the enthalpy difference between the return and supply air streams. Enthalpy may be suitably approximated by the wet bulb temperatures of the air streams. Using a first degree equation to calculate enthalpy from wet bulb temperatures between 6 and 18°C results in a maximum error of less than 2%, while using a second degree equation results in less than a half percent error for wet bulb temperatures between 4 and 20°C. By replacing the dry bulb temperature sensors with wet bulb sensors and adding some logic elements to the electronic circuitry, it is thus possible to measure cooling COP with the COP Meter.

Degree of simplicity in operation is the determining factor for the changes that are necessary to enable the COP Meter to be used as an anemometer. With the addition of one switch in the circuitry, a stop watch

and a sling psychrometer can be used to collect enough data to calculate air flow rate. The stop watch, sling psychrometer, and much of the calculation can be eliminated by more sophisticated electronics. Modifying the COP Meter to make it a continuous heat flow recorder is the simplest of the three options, for this requires only one additional switch in the circuitry and a slight change in operation procedure. Final package design, of course, will be dictated by user requirements and cost of these options.

Testing laboratories commonly use sophisticated instruments to measure electrical power input and heat flow and to calculate COP from these measurements. A Data Acquisition System (DAS) of this type is in use at the Tennessee Energy Conservation in Housing site in Knoxville, Tennessee. A multiprogrammable DAS in the Energy Conservation Laboratory at ORNL is also capable of calculating COP, but the heat flow measurements are made on the refrigerant circuit rather than on the air circuit. These systems are multipurpose units which do more than determine COP, and it is not feasible to use these systems on heat pumps installed and operating in the field. To the best of our knowledge, however, these multipurpose DAS systems are the nearest equivalent devices to the COP Meter that exist today.

Methods of determining heat pump COP are used by refrigeration mechanics that do not require the elaborate equipment used in testing laboratories. These methods, however, can result in significant errors in calculating COP; accuracy of heat flow measurement is generally directly proportional to the degree of instrumentation and to operator training. The COP Meter, on the other hand, performs repeatable laboratory grade COP measurements on installed units where only approximate measurements are now possible.

Do. Not Microfilm Distr.

ORNL/TM-8587
Dist. Category UC-95d

Internal Distribution

1. V. D. Baxter
2-6. V. R. Brantley
7. P. W. Childs
8. J. E. Christian
9. G. E. Courville
10. F. A. Creswick
11. R. D. Ellison
12. J. E. Farmer
13. T. D. Ferguson
14. S. K. Fischer
15. R. J. Friar
16. W. Fulkerson
17. K. S. Gaddis
18. L. D. Gilliam
19. D. S. Griffith
20. V. O. Haynes
21. K. E. Heidenreich
22. W. L. Jackson
23-72. D. W. Jared
73. M. L. Johnson
74. J. E. Jones Jr.
75. W. P. Levins
76. R. N. McGill
77. V. C. Mei
78. R. E. Mellon
79. J. W. Michel
80. D. R. Miller
81. R. E. Minturn
82. W. R. Mixon
83. J. C. Moyers
84. E. A. Nephew
85. H. Perez-Blanco
86. C. K. Rice
87. C. G. Rizy
88. R. C. Robertson
89. A. J. Shor
90. L. H. Thomas
91. H. E. Trammell
92. K. H. Vaughan
93. J. E. White
94. ORNL Patent Office
95. Central Research Library
96. Document Reference Section
97-98. Laboratory Records Department
99. Laboratory Records, RC

External Distribution

100. Institute of Energy Analysis, ORAU-Library, Oak Ridge, TN 37830
101. Roy Abbott, Advance Technology Operations, General Electric Company, AP6, Appliance Park, Louisville, KY 40225
102. John Adams, Whirlpool Corporation, Research & Engineering Center, Monte Road, Benton Harbor, MI 49022
103. Richard Alben, General Electric Company, Corporate R&D Center, Building K-1, Rm 5B37, P.O. Box 8, Schenectady, NY 12301
104. C. A. Allen, Energy Information Administration, EI-60, Federal Building, 1200 Pennsylvania Avenue N.W., Washington, DC 20461
105. Lawrence Ambs, Department of Mechanical Engineering, University of Massachusetts, Amherst, MA 01003
106. James Barker, ARCO Ventures Company, 911 Wishire Boulevard, Box 2679-TA, Los Angeles, CA 90051
107. E. K. Bastress, Energy Conversion & Utilization Technology Division, CS-142, Forrestal Building, Department of Energy, Washington, DC 20585
108. A. F. Bedinger, 1128 Keowee Ave., Knoxville, TN 37919
109. A. F. Bedinger, Jr., 3847 Keowee Ave., Knoxville, TN 37919

110. Morton Blatt, 1200 Prospect Street, P.O. Box 2351, LaJolla, CA 92038
111. Peter Bodett, Duo-Therm Division, Motor Wheel Corporation, LaGrange, IN 46761
112. Ulrich Bonne, Honeywell Incorporated, 10701 Lyndale Avenue South, Corporate Technology Center, Materials & Processes Department, Bloomington, MN 55420
113. Arne Boysen, Jarntorget 78, 111 29 Stockholm, Sweden
114. Joseph Braymer, Mechanical & Aerospace Engineering Department, Case Western Reserve, University Circle, Cleveland, OH 44106
115. James Brisee, North Carolina Energy Institute, Department of Commerce, P.O. Box 12235, Research Triangle Pk., NC 27709
116. J. Robert Cairns, University of Michigan Dearborn, School of Engineering, Department of Mechanical Engineering, Dearborn, MI 48128
117. Jim Calm, Energy Management & Utilization Division, Electric Power Research Institute, Heat Pump Development, P.O. Box 10412, Palo Alto, CA 94303
118. Joe Canal, General Electric Company, Troup Highway, Tyler, TX 75711
119. C. Gerald Carrington, University of Aston in Birmingham, Department of Physics, Birmingham, England
120. Tom J. Cebulla, Honeywell Incorporated, 1700 W. Hwy 36, MN 19 T470, Roseville, MN 55113
121. Roger Chesebro, Westinghouse Electric Corporation, Research & Development Center, 1310 Beulah Road, Pittsburg, PA 15235
122. Raymond Cohen, Ray W. Herrich Laboratories, Purdue University, West Lafayette, IN 47907
123. V. I. Conley, Virginia Polytechnic Institute & State University, Department of Mechanical Engineering, Blacksburg, VA 24061
124. Ken Cooper, York Division, Borg-Warner Corporation, P.O. Box 1592, York, PA 17405
125. James Crawford, Manager, Advanced Systems, General Electric Company, 6200 Troup Highway, Tyler, TX 75711
126. Ali Dabiri, Science Applications, Inc., 1200 Prospect Street, P.O. Box 2351, LaJolla, CA 92038
127. Thomas Dean, University of Kansas, Lawrence, KS 66045
128. Irvin Derks, Manager Engineering Development, Bard Manufacturing Company, Bryan, OH 43506
129. David Didion, Mechanical Systems Section, Building Environment Division, National Bureau of Standards, Building 226, Room B126, Washington DC 20234
130. Albert Domingorena, Carrier Corporation, Building TR-4, Carrier Parkway, Post Office Box 4808, Syracuse, NY 13221
131. Alan Drucker, Consumer Products Division, Carrier Corporation, Syracuse, NY 13221
132. G. D. Duffy, Air Conditioning News, P.O. Box 2600, Troy, MI 48084
133. Alex Dybbs, Case Western Reserve University, Glennan Building, Cleveland, OH 44106
134. Amir Ecker, Northrup, Inc., 302 Nichols Drive, Hutchins, TX 75141

135. Thomas Edwards, The Rovac Corporation, 100 Rovac Parkway, Rockledge, FL 32955
136. Donald Elger, Department of Mechanical Engineering, Oregon State University, Corvallis, OR 97331
137. A. H. Elmahdy, Energy and Services Section, National Research Council, Division of Building Research, Ottawa, Canada
138. Richard Erth, York Division, Borg-Warner, P.O. Box 1592, York, PA 17405
139. J. N. Eustis, Department of Energy, Office of Industrial Programs, CE-121.1, 1000 Independence Avenue S.W., Washington, DC 20585
140. Scott Farley, The Coleman Company, Inc., Special Products Group, 250 North St. Francis, Wichita, KS 67201
141. Arthur Fellerman, McQuay Group, 13600 Ind. Park Boulevard, Minneapolis, MN 55440
142. Robert Fischer, Battelle-Columbus Laboratory, 505 King Avenue, Columbus, OH 43201
143. R. J. Fiskum, Energy Conversion Equipment Branch, CE-113.2, Department of Energy, 1000 Independence Avenue S.W., Washington, DC 20585
144. Albert Fox, Texas Instruments, Inc., P.O. Box 1255, MS 3531, Johnson City, TN 37601
145. G. W. Gatecliff, Research Laboratory, Tecumseh Products Company, Ann Arbor, MI 48105
146. Tom Gertz, General Electric Company, 6200 Troup Highway, Tyler, TX 75711
147. J. H. Gibbons, Office of Technology Assessment, U.S. Congress, 600 Pennsylvania Avenue S.E., Washington, DC 20510
148. Paul Glamm, The Trane Company, 3600 Pammell Creek Road, LaCrosse, WI 54601
149. L. R. Glicksman, Massachusetts Institute of Technology, 77 Massachusetts Avenue, Building 3-137, Cambridge, MA 02139
150. Alan Glover, School of Engineering, Mechanical Engineering Department, University of Auckland, Auckland, New Zealand
151. S. D. Goldstein, Advanced Energy Systems, Exxon Enterprises, Inc., Post Office Box 192, Florham Park, NJ 07932
152. R. Eugene Goodson, Hoover Universal, Inc., P.O. Box 1003, 825 Victors Way, Ann Arbor, MI 48106
153. Richard Greenhaus, 256 Washington Street, Mount Vernon, NY 10550
154. D. E. Grether, International Environmental Corporation, 5000 S.W. 7th Street, Oklahoma City, OK 73125
155. Russ Griffith, Copeland Corporation, Campbell Road, Sidney, OH 45365
156. G. C. Groff, Research Division, Carrier Corporation, Syracuse, NY 13201
157. John Hackstedde, Tecumseh Products Company, Tecumseh, MI 49236
158. R. Hanski, Studsvik Energiteknik AB, S-611 82 Nykioping, Sweden
159. Gordon Hart, Owens-Corning Fiberglass Technical Center, Granville, OH 43023
160. Wayne Helmer, Southern Illinois University at Carbondale, School of Engineering & Tech., Department of Thermal & Environmental Engineering, Carbondale, IL 62901

161. R. J. Hemphill, Gas Research Institute, 8600 Bryn Mawr Avenue, Residential & Commercial Utilization, Chicago, IL 60631
162. Arlo Hendrickson, General Electric Company, Troup Highway, Tyler, TX 75711
163. James Hill, Thermal Solar Program, National Bureau of Standards, Washington DC 20234
164. C. C. Hiller, Sandia Laboratories, Livermore, CA 94550
165. Larry Hobart, American Public Power Association, 2000 Virginia Avenue N.W., Washington, DC 20037
166. E. C. Hise, 106 E. Irving Lane, Oak Ridge, TN 37830
167. Tina Hobson, Building Equipment Division, CE-113.2, Department of Energy, 1000 Independence Avenue S.W., Washington, DC 20585
168. David Hodgett, Battelle-Instut e. V., Am Romerhof 35, Postfach 900160, 6000 Fankfurt am Main 90, West Germany
169. Allen Holman, Mechanical Data, 215 Center Park Drive, Suite 100, Knoxville, TN 37922
170. Fred Honnold, Consumer Products Division, Carrier Corporation, Syracuse, NY 13201
171. Michael Hughes, Friedrich Air Conditioning & Refrigeration, 2000 W. Commercial Boulevard, Fort Lauderdale, FL 22209
172. Bao Hwang, David Taylor Naval Ship R&D Center, Mail Code 2722, U.S. Naval Academy, Annapolis, MD 21402
173. Howard Izawa, InterNorth, Inc., Northern Gas Company, 4840 F Street, Omaha, NB 68117
174. Richard Jacobson, Honeywell Inc., 10701 Lyndale Avenue South, Bloomington, MN 55420
175. T. Jacoby, Tecumseh Products Company, Tecumseh, MI 49286
176. H. Jaster, General Electric Corporate Research & Development, General Electric Company, P.O. Box 43, Schenectady, NY 13201
177. P. L. Johnson, Oak Ridge Associated Universities, Executive Office, Administration Building, Oak Ridge, TN 37830
178. F. R. Kalhammer, Energy Management and Utilization Division, Electric Power Research Institute, 3412 Hillview Avenue, P.O. Box 10412, Palo Alto, CA 94303
179. F. Kalivoda, Copeland Corporation, Sydney, OH 45365
180. Mark Kalman, E-Tech Incorporated, 3570 American Drive, Atlanta, GA 30341
181. Rube Kelto, Tecumseh Products Company, Tecumseh, MI 49286
182. R. W. King, Manager, Advanced Engineering, Copeland Corporation, Sydney, OH 45365
183. Sandford Klein, University of Wisconsin, Mechanical Engineering, Madison, WI 53706
184. Ira Krepchin, Foster-Miller Associates, Inc., Engineers, 350 Second Avenue, Waltham, MA 02154
185. H. Kruse, University Hannover, Welfengarten 1 A Hannover, West Germany
186. Stephen Kugle, University of Texas at Arlington, Department of Mechanical Engineering, P.O. Box 19023, Arlington, TX 76019
187. Todd LaPorte, Institute of Government Studies, University of California, Berkeley, CA 94720
188. Arvo Lannus, Residential & Commercial Applications, Electric Power Research Institute, 3412 Hillview Avenue, P.O. Box 10412, Palo Alto, CA 94303

189. James W. Leach, Department of Mechanical & Aerospace Engineering, Department of Engineering, North Carolina State University, P.O. Box 5246, Raleigh, NC 27650
190. Dr. Y. N. Lee, Roy C. Ingersoll Research Center, Wolf & Algonquin Roads, Borg-Warner Corporation, Des Plaines, IL 60018
191. W. David Lee, Arthur D. Little, Inc., Acorn Park, Cambridge, MA 02140
192. Clayton Lemal, Low Temperature Laboratory, Division of Mechanical Engineering, Montreal Road, Ottawa, Canada K1A OR6
193. Ian Lewis, Middleton Associates, 980 Yonge Street, Suite 404, Toronto, Canada M4W2J9
194. A. W. Liles, EXXON Enterprises Inc., P.O. Box 192, Florham Park, NJ 07932
195. D. C. Lim, Energy Conversion Equipment Branch, CE-113.2, Department of Energy, 1000 Independence Avenue S.W., Washington, DC 20585
196. R. A. Lucheta, Westinghouse Electric Corporation, Research & Development Center, 1310 Beulah Road, Pittsburg, PA 15235
197. H. P. Luckett, Editor in Chief, Popular Science, 380 Madison Avenue, New York, NY 10017
198. Ward MacArthur, Honeywell Inc., 2600 Ridgeway Parkway, Minneapolis, MN 55413
199. J. F. T. MacLaren, University of Strathclyde, Glasgow, Scotland
200. Robert Mauro, Energy Management & Utilization Division, Electric Power Research Institute, 3412 Hillview Avenue, P.O. Box 10412, Palo Alto, CA 94304
201. Jim McCallum, Executive Editor, Air Conditioning & Refrig. Business, 614 Superior Avenue W., Cleveland, OH 44113
202. E. A. McPherson, SED Systems Ltd., P.O. Box 1464, Saskatoon, Saskatchewan, Canada S7K3P7
203. F. C. McQuiston, Oklahoma State University, 301 Engineering North, Stillwater, OK 74074
204. Philip Metz, Brookhaven National Laboratory, Upton, NY 11973
205. Mark Middleton, Columbus Products Company, 300 Phillipi Road, Columbus, OH 43228
206. R. Scott Miller, General Electric Company, CRD-River Road, Building #37-615, Schenectady, NY 12345
207. J. P. Millhone, Office of Buildings Energy Research & Development, CE-11, Department of Energy, 1000 Independence Avenue S.W., Washington, DC 20585
208. F. H. Morse, Office of Solar Heat Technologies, CE-31, Department of Energy, 1000 Independence Avenue S.W., Washington, DC 20585
209. Robert Morse, Tecumseh Products Company, Tecumseh, MI 49286
210. Larry Moss, P.O. Box 1496, Estes Park, CO 80517
211. Neno Nenov, Linde Division, Union Carbide Corporation, Tonawanda, NY 14150
212. Van-Thanh Nguyen, Mitre Corporation, Metreck Division, 1820 Dolley Madison Boulevard, McLean, VA 22102
213. Dennis O'Neal, 400 N. River Road, Apartment 603, West Lafayette, IN 47906

214. Mark Oven, Foster-Miller Associates, Inc., 350 Second Avenue, Waltham, MA 02154
215. Andrew W. Paczuski, Principle Engineer, Bristol Compressors, Bristol, VA
216. Jerald Parker, School of Mechanical & Aerospace Engineering, Oklahoma State University, 218 Engineer North, Stillwater, OK 74074
217. A. Patani, Honeywell Inc., 10701 Lyndale Avenue South, Bloomington, MN 55420
218. Michael Perlsweig, Division of Conservation Research and Technology, Department of Energy, 20 Massachusetts Avenue N.W., Washington DC 20545
219. Lawrence Peterson, 1671 S.W. Fairhill, Roseburg, OR 97470
220. B. J. Pleiss, A. O. Smith Corporation, 531 North 4th Street, Tipp City, OH 45371
221. Lee Preston, A. O. Smith Corporation, 531 North 4th Street, Tipp City, OH 45371
222. T. Ratchford, Committee on Science and Technology, Subcommittee on Energy Research and Development, House of Representatives, Washington, DC 20515
223. Wayne Reedy, Carrier Corporation, Carrier Parkway, Syracuse, NY 13221
224. Gordon Reistad, Oregon State University, Department of Mechanical Engineering, Corvallis, OR 97331
225. Patrick Reynolds, Mechanical Technology Inc., 968 Albany-Shaker Road, Latham, NY 12110
226. Steve Riedel, General Electric Company, Fort Wayne, IN
227. Bill Riley, Advance Development, Heil Quaker Corporation, 647 Thompson Lane, P.O. Box 40566, Nashville, TN 37204
228. Mike Riley, General Electric Company, AP6-227, Appliance Park, Louisville, KY 40225
229. J. Rizzuto, New York State Energy Research & Development Authorization, Agency Building No. 2, Empire State Plaza, Albany, NY 12223
230. J. H. Rothenburg, Utilities Systems, Department of Housing & Urban Development, 451 Seventh Street S.W., Washington, DC 20410
231. J. D. Ryan, Energy Conversion Equipment Branch, CE-113.2, Department of Energy, 1000 Independence Avenue S.W., Washington, DC 20585
232. L. A. Sarkes, American Gas Association, 1515 Wilson Boulevard, Arlington, VA 22209
233. M. L. Savitz, Deputy Assistant Secretary for Conservation, CE-10, Department of Energy, 1000 Independence Avenue S.W., Washington, DC 20585
234. D. E. Scherpereel, Director, Mechanical Systems Research, Elisha Gray II -, Research & Engineering Center, Monte Road, Benton Harbor, MI 49022
235. Carl Schmittle, York Division, Borg-Warner, York, PA 17405
236. Robert Schoenhals, Department of Mechanical Engineering, Purdue University, West Lafayette, IN 47907

237. Mark Schuetz, AMTI, 141 California Street, Newton, MA 02158
238. James Schulze, Technology Program Manager, General Electric Company, Appliance Park, Building 6, Room 244, Louisville, KY 40225
239. T. C. Scott, Department of Mechanical & Aerospace Engineering, University of Virginia, Charlottesville, VA 22901
240. Musoke Sendanla, Tennessee Valley Authority, Electrical Systems, 1150 Chestnut Street Tower II, Chattanooga, TN 37401
241. Takao Senshu, Mechanical Engineering Research Laboratory, Hitachi, Ltd., 390 Muramatsu, Shimizu-shi, Shizuoka-ken, Japan
242. Michael Sexton, Department of Mechanical & Aerospace Engineering, University of Virginia, Charlottesville, VA 22901
243. Ramesh Shah, Harrison Radiator Division, General Motors Corporation, Lockport, NY 14094
244. Samuel Shelton, School of Mechanical Engineering, Georgia Institute of Technology, Atlanta, GA 30332
245. D. E. Sherpereel, Research and Engineering Center, Whirlpool Corporation, Benton Harbor, MI 49022
246. Tony Sigmon, Research Triangle Institute, Energy & Environmental Research, P.O. Box 12194, Research Triangle Pk., NC 27709
247. George Simmons, University of Idaho, College of Engineering, Department of Chemical Engineering, Buchanan Engineering Laboratory 308, Moscow, ID 83843
248. G. G. Slaughter, 240 N. Purdue Ave., Oak Ridge, TN 37830
249. J. A. Smith, Test and Evaluation Branch, CE-113.2, Department of Energy, 1000 Independence Avenue S.W., Washington, DC 20585
250. Dr. Yates Sorrell, N. C. Alternative Energy Corporation, P.O. Box 12699, Research Triangle Pk., NC 27709
251. Dr. Yates Sorrell, N. C. Alternative Energy Corporatioon, P.O. Box 12699, Research Triangle Pk., NC 27709
252. E. W. Spannhake, 514 Turtlehatch Road, Naples, FL 33940
253. K. E. Starner, Advance Engineering, York Division, Borg-Warner Corporation, P.O. Box 1592, York, PA 17405
254. John Stephenson, University of Auckland, Auckland, New Zealand
255. W. F. Stoecker, University of Illinois Urbana-Champaign, Department of Mechanical & Indus. Engineering, 144 Mechanical Engineering Building, Urbana, IL 61801
256. Robert Stricker, The Rovac Corporation, 100 Rovac Parkway, Rockledge, FL 32955
257. Shiv Sud, Strategic Planning and Analysis Group, Ministry of Energy, 56 Wellesley Street West, Queen's Park, Toronto, Canada
258. W. D. Syniuta, Advanced Mechanical Technology, Inc., 141 California Street, Newton, MA 02158
259. C. C. Thiel, Jr., Division of Advanced Technology Applications, National Science Foundation, 1800 G. Street N.W., Washington, DC 20550
260. W. H. Thielbahr, Energy Conservation Branch, Department of Energy, Idaho Operations Office, 550 Second Street, Idaho Falls, ID 83401
261. W. C. Thomas, Virginia Polytechnic Institute & State University, Blacksburg, VA 24061
262. William Toscano, Foster-Miller Associates, 135 Second Avenue, Waltham, MA 02154

263. D. Tree, Ray Herrick Laboratory, Purdue University, West Lafayette, IN 47907
264. Dutch Uselton, Northrup Incorporation, 302 Nichols Drive, Hutchins, TX 75141
265. F. Vahid, University of Newcastle Upon Tyne, Building Science Section, School of Architecture, Newcastle Upon Tyne, England
266. Himanshu Vakil, General Electric Corporate R&D, P.O. Box 8, Schenectady, NY 12301
267. Hendrik Van Der Ree, TNO, Heat Pump Section, Laan Van Westenenk 501, Apeldoorn, The Netherlands
268. S. E. Veyo, Westinghouse Electric Corporation, Research & Development Center, 1310 Beulah Road, Pittsburg, PA 15235
269. D. J. Walukas, Foster-Miller Associates, Inc., 795 Oak Ridge Turnpike, Oak Ridge, TN 37830
270. Andy Wan, Room EM204, U.S. Department of Commerce, National Bureau of Standards, Washington DC 20234
271. Bernie Warning, Friedrich A. C. & R., 4200 N. Pan Am Expressway, P.O. Box 1540, San Antonio, TX 78295
272. Ralph Webb, Department of Mechanical Engineering, Pennsylvania State University, 208 Mechanical Engineering Building, University Park, PA 16802
273. C. H. Weight, Elf Aquitaine Development, 9 West 57th Street, New York, NY 10019
274. David Wensky, Copeland Corporation, 250 East Wilson Bridge Rd., Suite 255, Worthington, OH 43085
275. M. Wilden, University of New Mexico, Albuquerque, NM 87115
276. J. C. Wilson, Carlyle Compressor Company, 4803, Syracuse, NY 13221
277. Les Wright, Project Manager, Residential Space Conditions System, 8600 W. Bryn Mawr Avenue, 10 West 35th Street, Chicago, IL 60631
278. George Yamahoto, ETL Testing Laboratory, Inc., Industrial Park, Cortland, NY 13045
279. Hiromu Yasuda, Mechanical Engineering Research Laboratory, Hitachi, Ltd., 390 Muramatsu, Shimizu-shi, Shizuoka-ken, Japan
280. T. Yoshii, Mitsubishi Heavy Industries America, Inc., Suite 2101 John Hancock Center, 875 North Michigan Avenue, Chicago, IL 60611
281. David Young, Ontario Hydro, Research Division, 800 Kipling Avenue, Toronto, Canada M8Z 5S4
282. Ronald Zerkle, University of Cincinnati, Cincinnati, OH
283. R. V. Zigler, General Electric Company, 570 E. 16th, Holland, MI 49423
284. Congressional Information Service, Research Building 83, Kodak Park, Rochester, NY 14050
285. Edison Electric Institute, 8th Floor, 1111 19th Street N.W., Washington, DC 20036
286. Office of the Assistant Manager for Energy Research and Development, U.S. Department of Energy, Oak Ridge Operations, Oak Ridge, TN 37830
287. Energy Conservation Distribution, Oak Ridge National Laboratory, Building 9102-2, Rm. 112, Oak Ridge, TN 37830

288-529. Given distribution as shown in DOE/TIC-4500 under category UC-95d (Energy Conservation - Buildings and Community Systems)

☆ U.S. GOVERNMENT PRINTING OFFICE: 1983-646-055/253